

Electronic Supplementary Information for

**Development of ^{18}F -Labeled Azobenzothiazole Tracer for α -Synuclein Aggregates in the
Brain**

Jiajun Wu^a, Meiting Mao,^a Jie Yang,^a Kexin Li,^a Pengxin Deng,^a Jing Zhong,^a Xiaoi Wu,^{b,*}
and Yan Cheng^{a,*}

^aKey Laboratory of Drug-Targeting and Drug Delivery System of the Education Ministry and Sichuan Province, Sichuan Engineering Laboratory for Plant-Sourced Drug and Sichuan Research Center for Drug Precision Industrial Technology, West China School of Pharmacy, Sichuan University, Chengdu, 610041, China

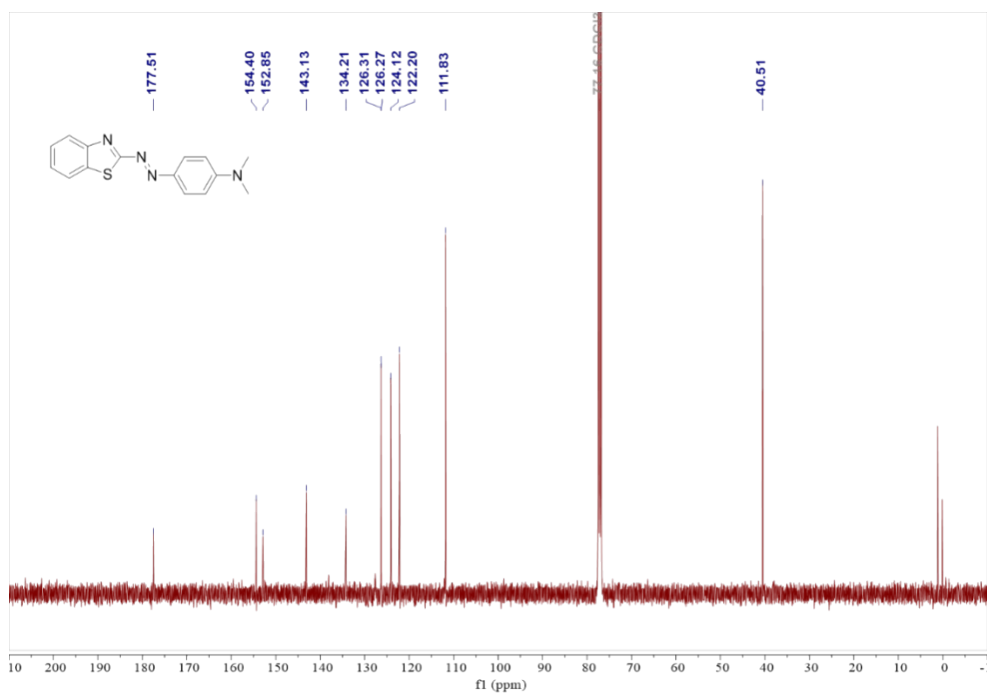
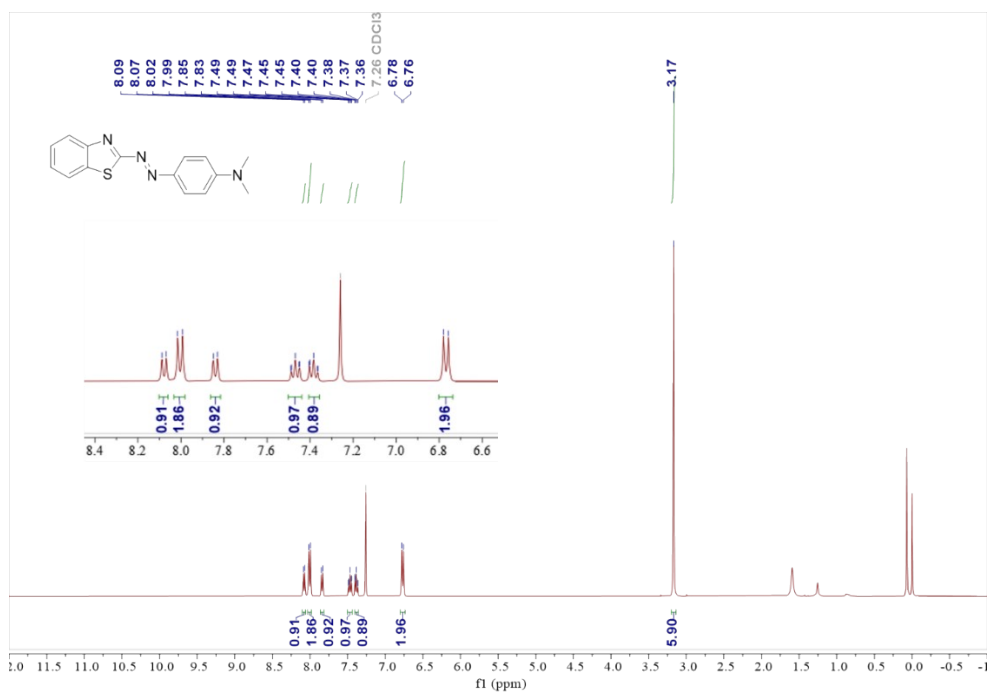
^bDepartment of Nuclear Medicine, West China Hospital, Sichuan University, Chengdu, 610041, China

*To whom correspondence should be addressed: e-mail: yancheng@scu.edu.cn for Y. Cheng;
xiaoi.wu@scu.edu.cn for X. Wu.

Table of Contents

1. Chemistry	S3
2. HPLC Purity	S17
3. Optical Measurements	S25
4. Preparation of Protein Aggregates.....	S30
5. Spectral Measurements with Protein Aggregates in Solutions.....	S31
6. Fluorescence Staining of Brain Sections.....	S31
7. Saturation Binding Assays of NN-F.....	S34
8. Stability Studies.....	S34
References	S35

1. Chemistry



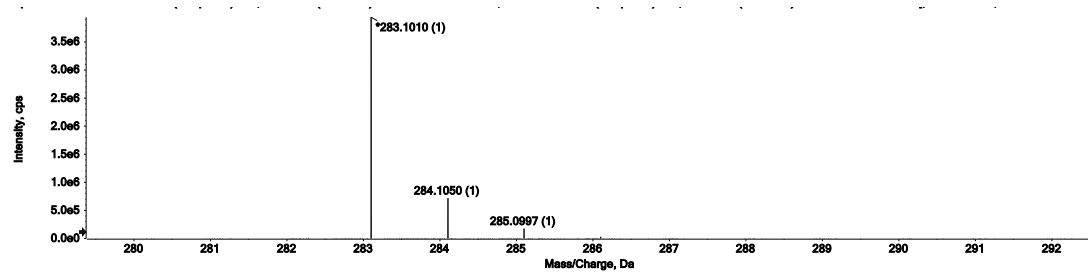
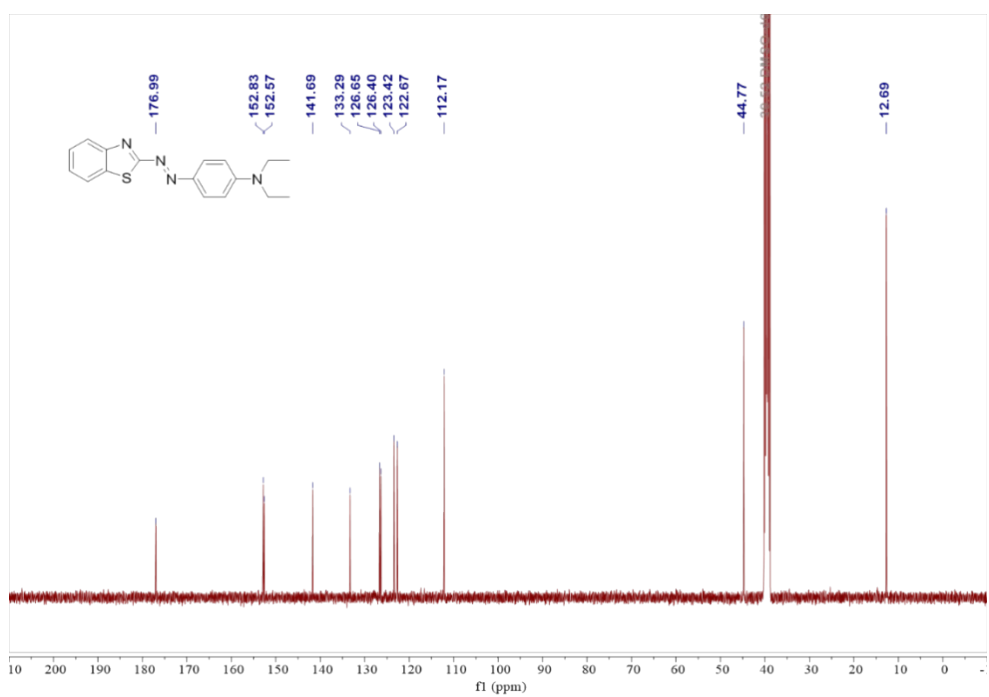
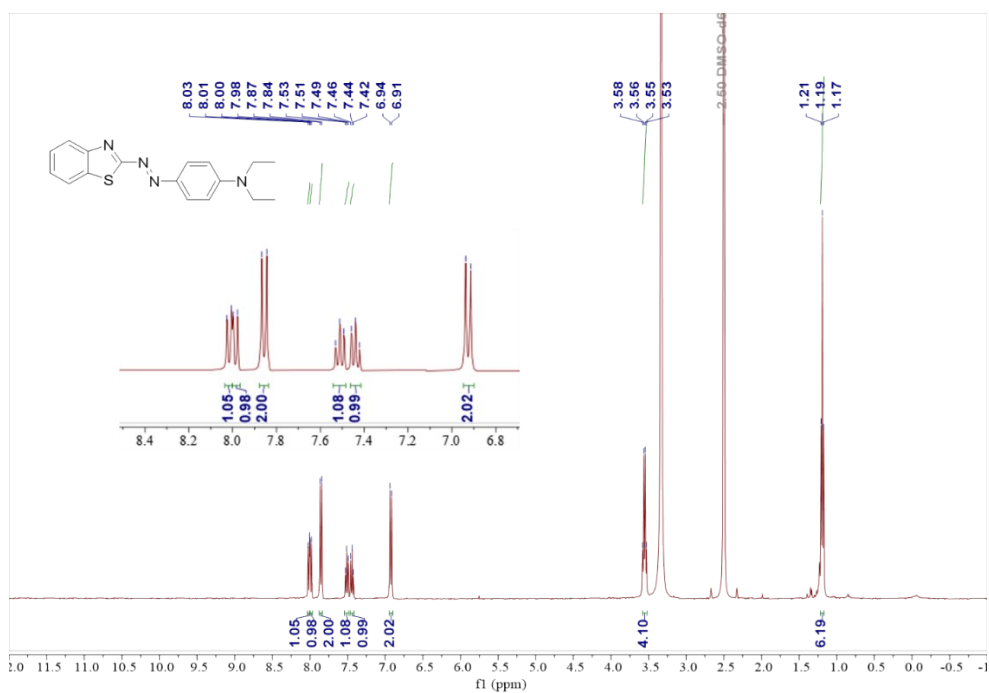


Fig. S1 ^1H NMR, ^{13}C NMR, and HRMS spectra of NN-Me.



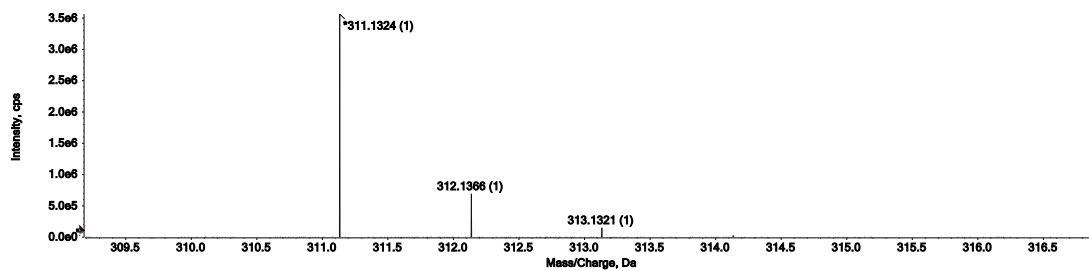
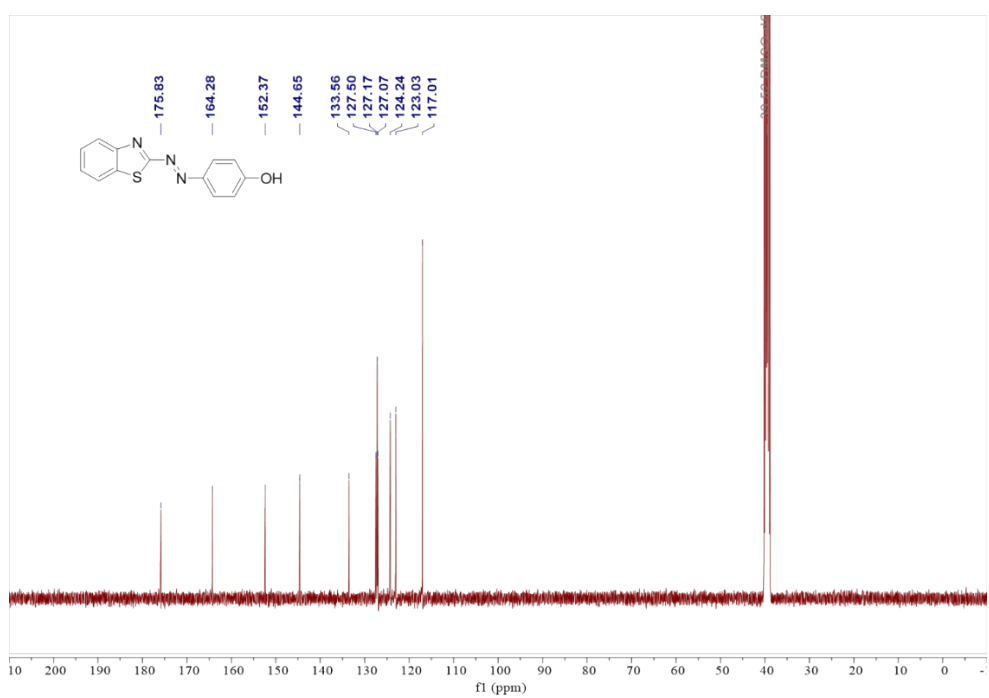
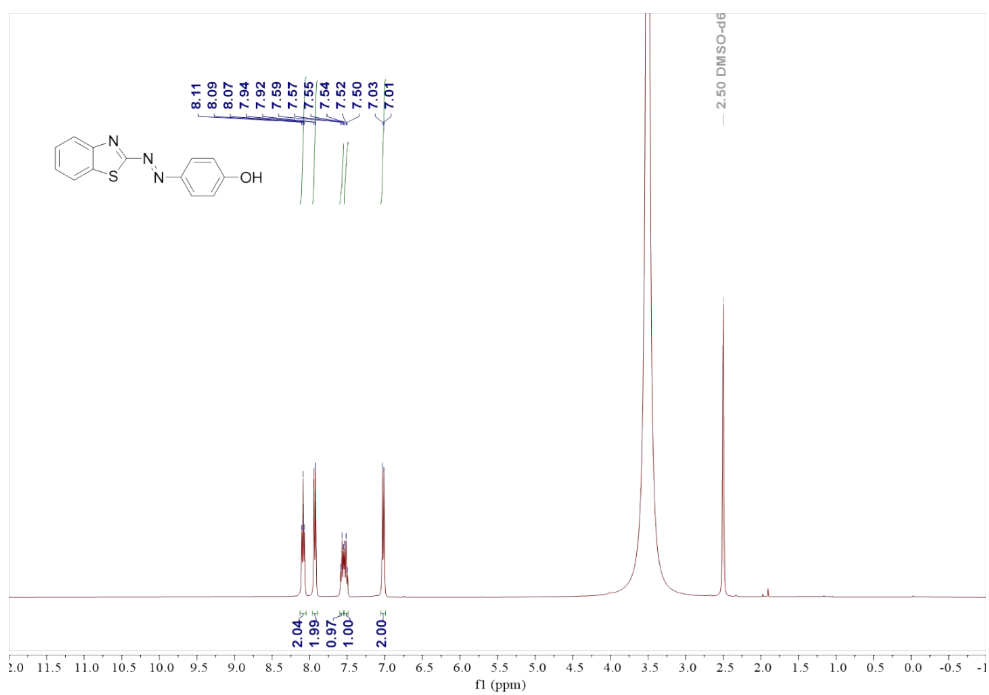


Fig. S2 ^1H NMR, ^{13}C NMR, and HRMS spectra of NN-Et.



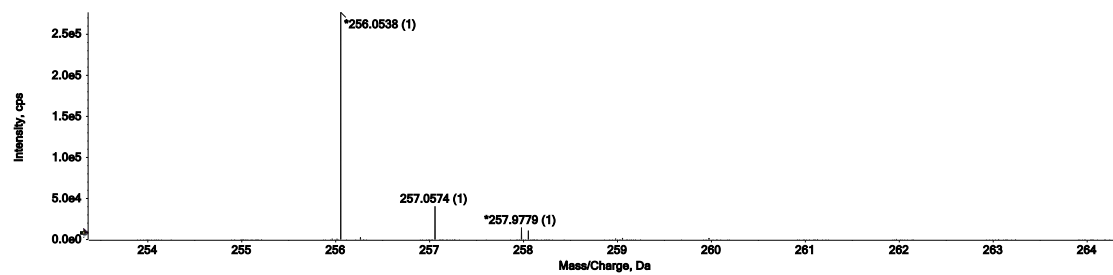
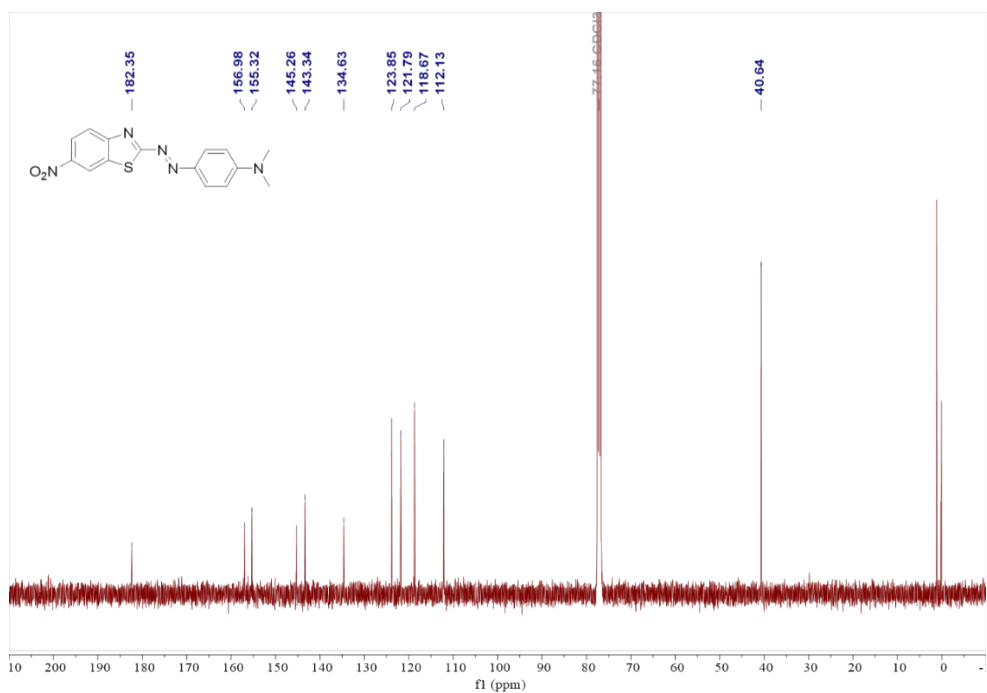
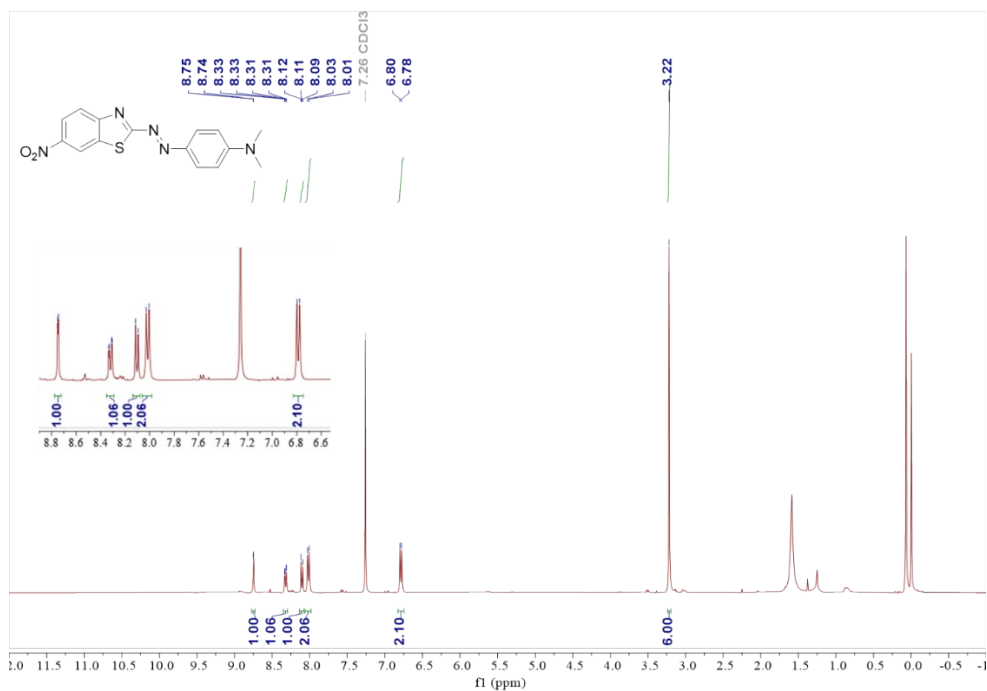


Fig. S3 ^1H NMR, ^{13}C NMR, and HRMS spectra of NN-OH.



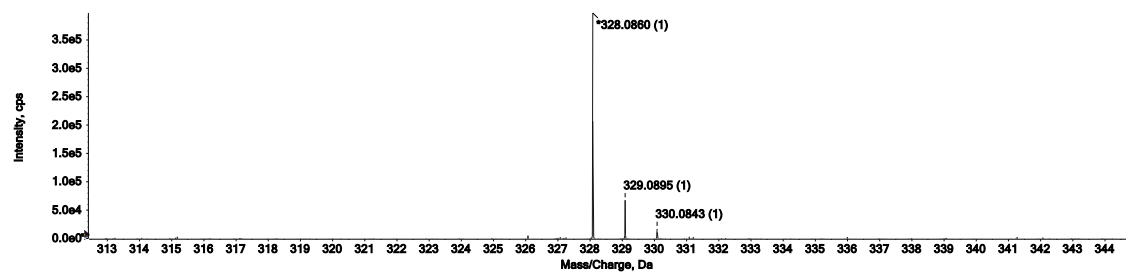
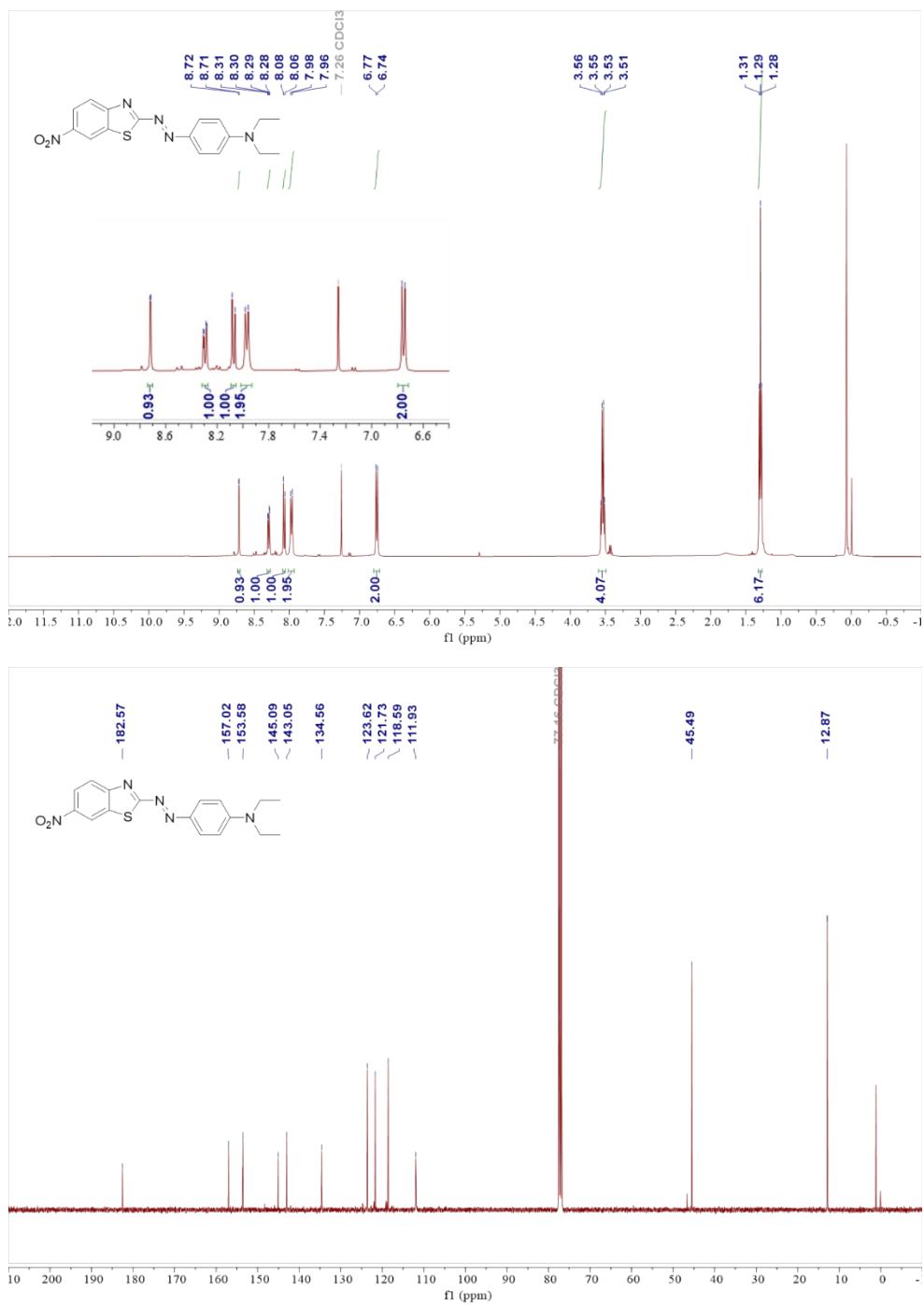


Fig. S4 ^1H NMR, ^{13}C NMR, and HRMS spectra of NiNN-Me.



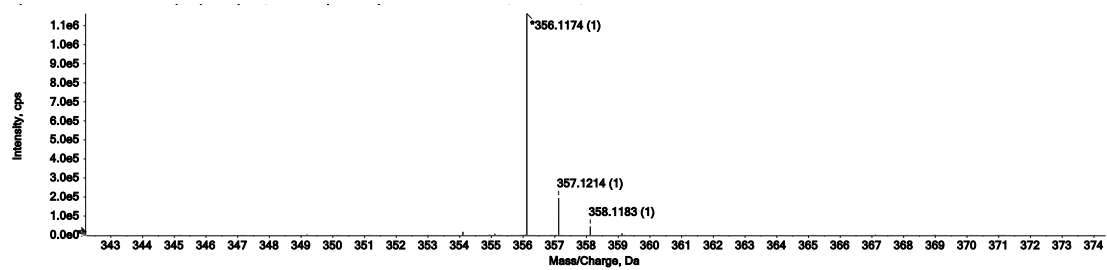
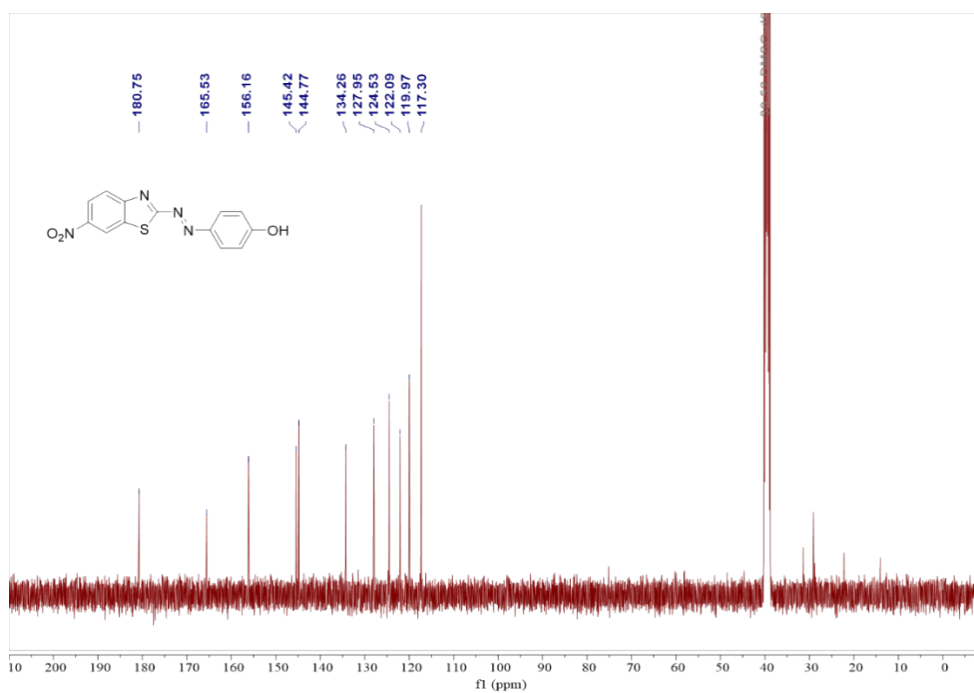
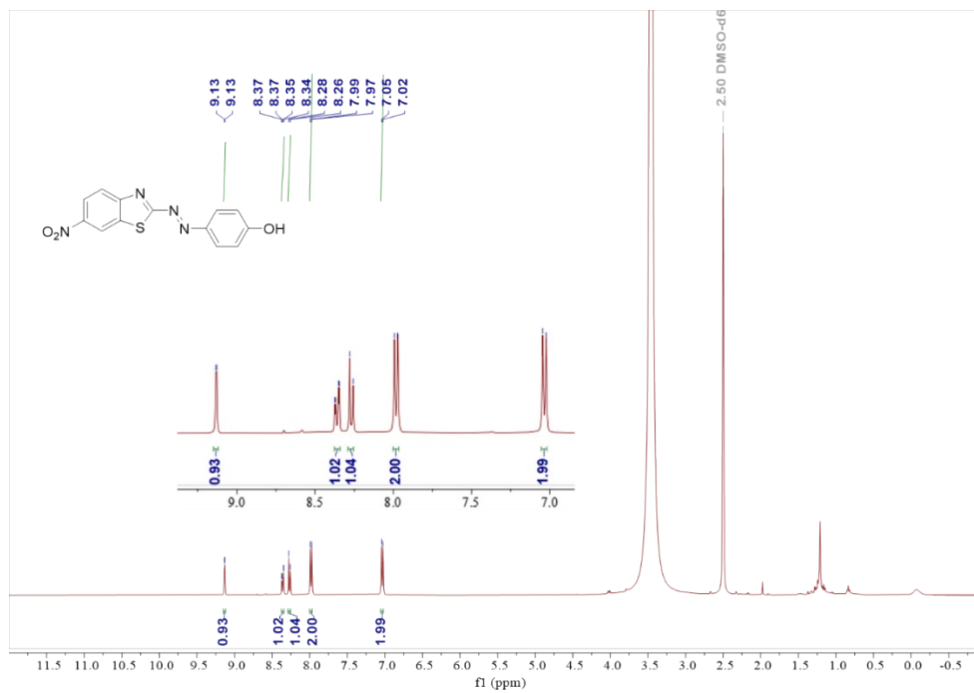


Fig. S5 ^1H NMR, ^{13}C NMR, and HRMS spectra of NiNN-Et.



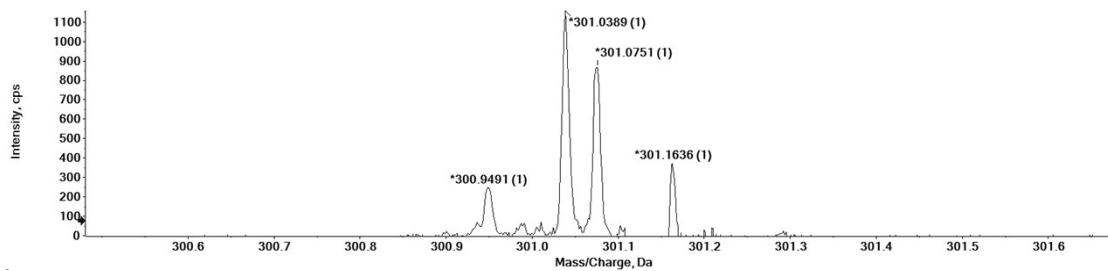
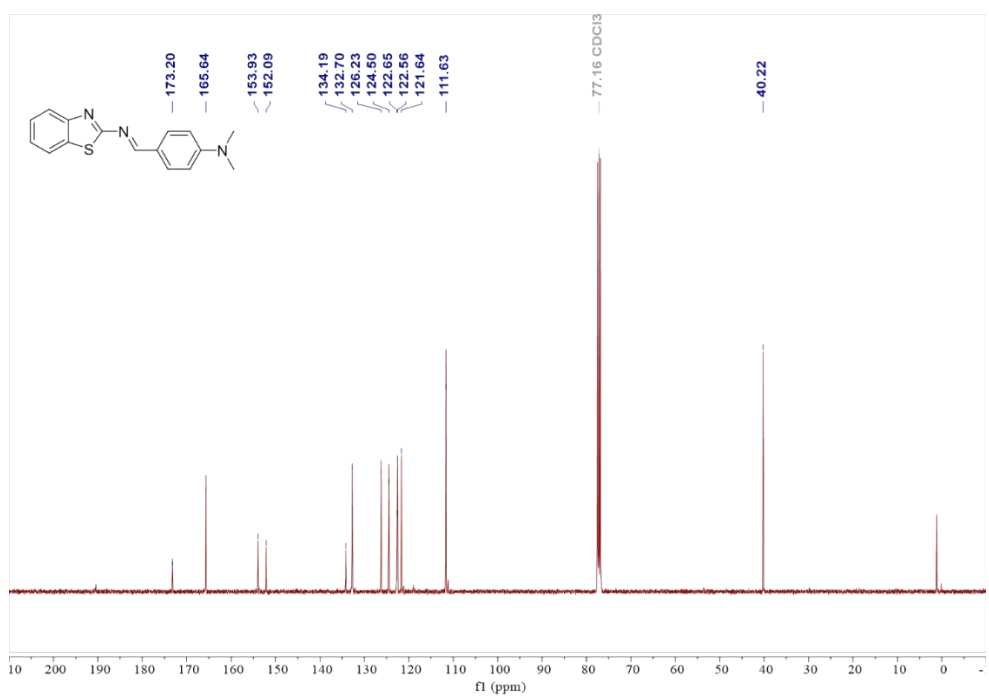
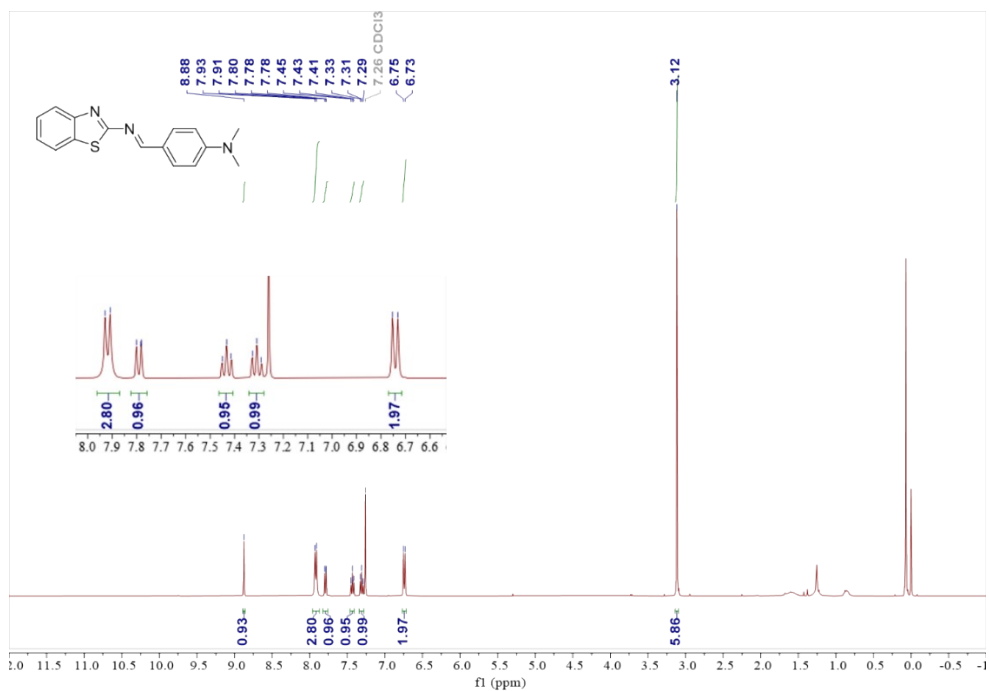


Fig. S6 ^1H NMR, ^{13}C NMR, and HRMS spectra of NiNN-OH.



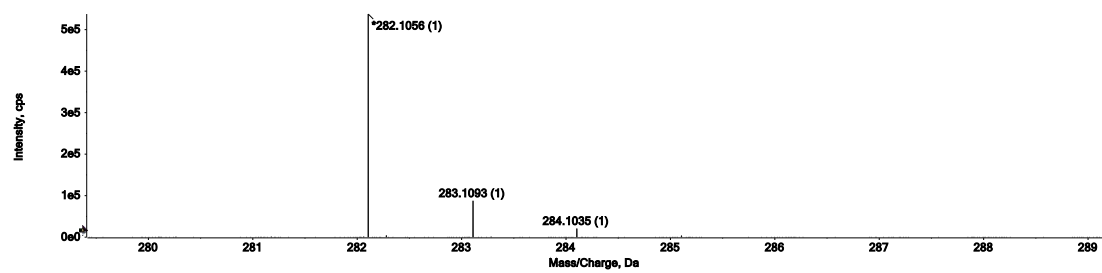
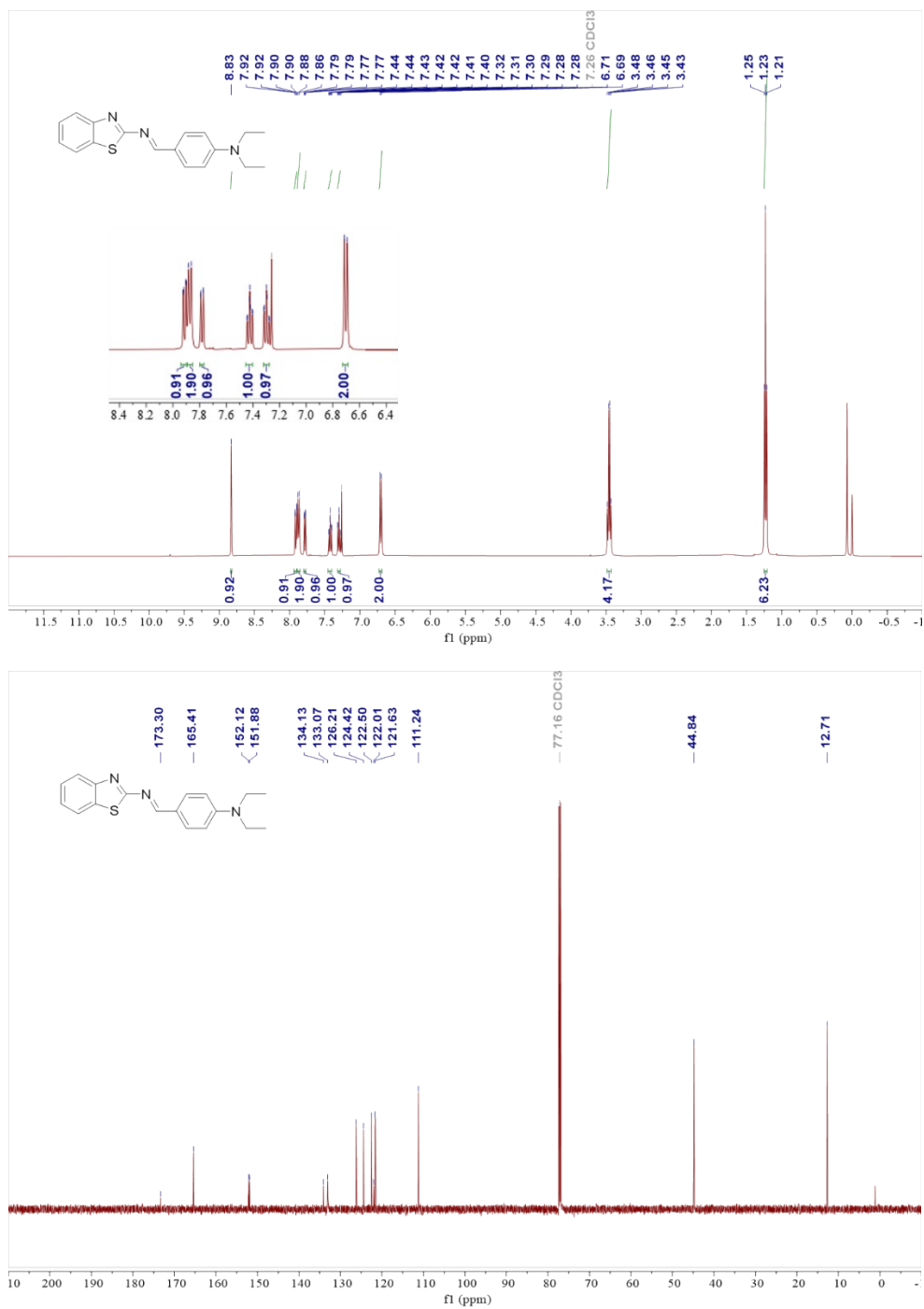


Fig. S7 ^1H NMR, ^{13}C NMR, and HRMS spectra of NC-Me.



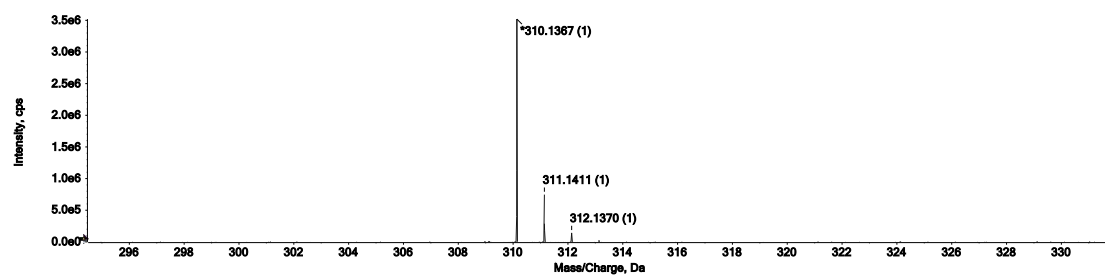
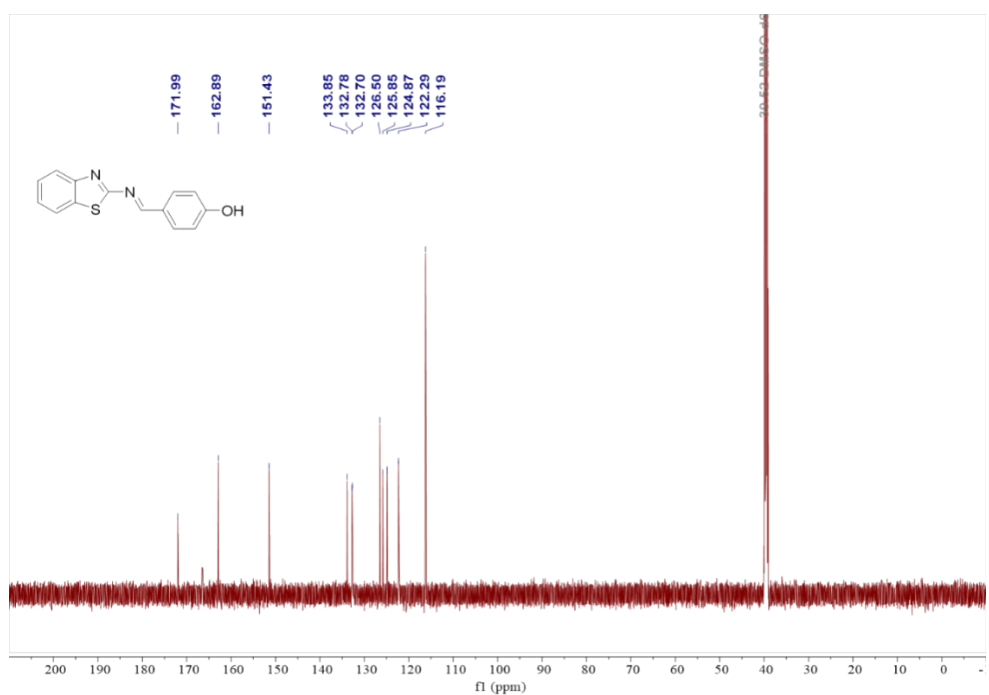
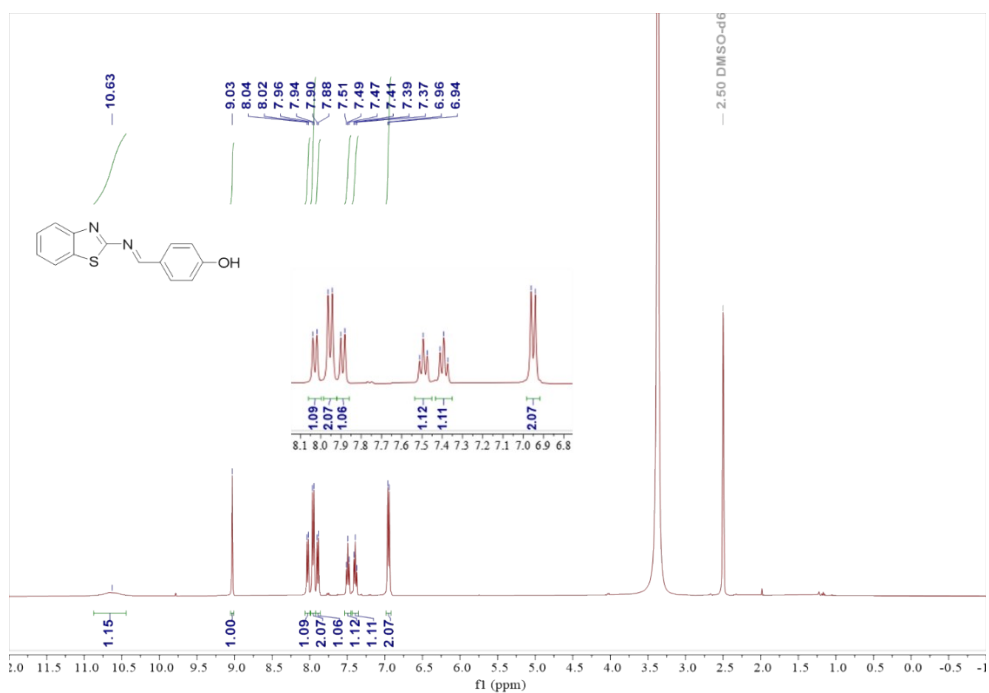


Fig. S8 ^1H NMR, ^{13}C NMR, and HRMS spectra of NC-Et.



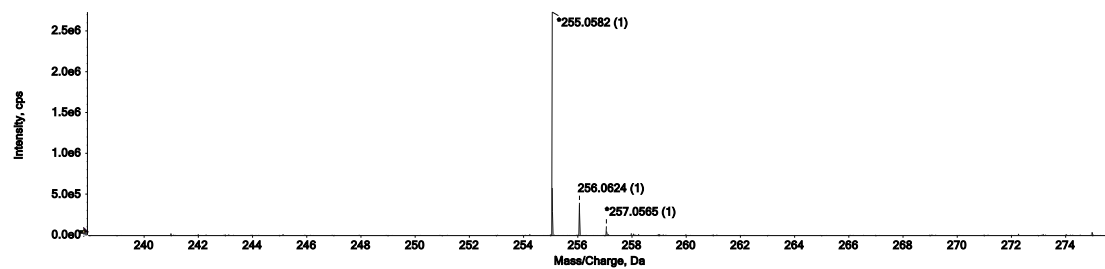
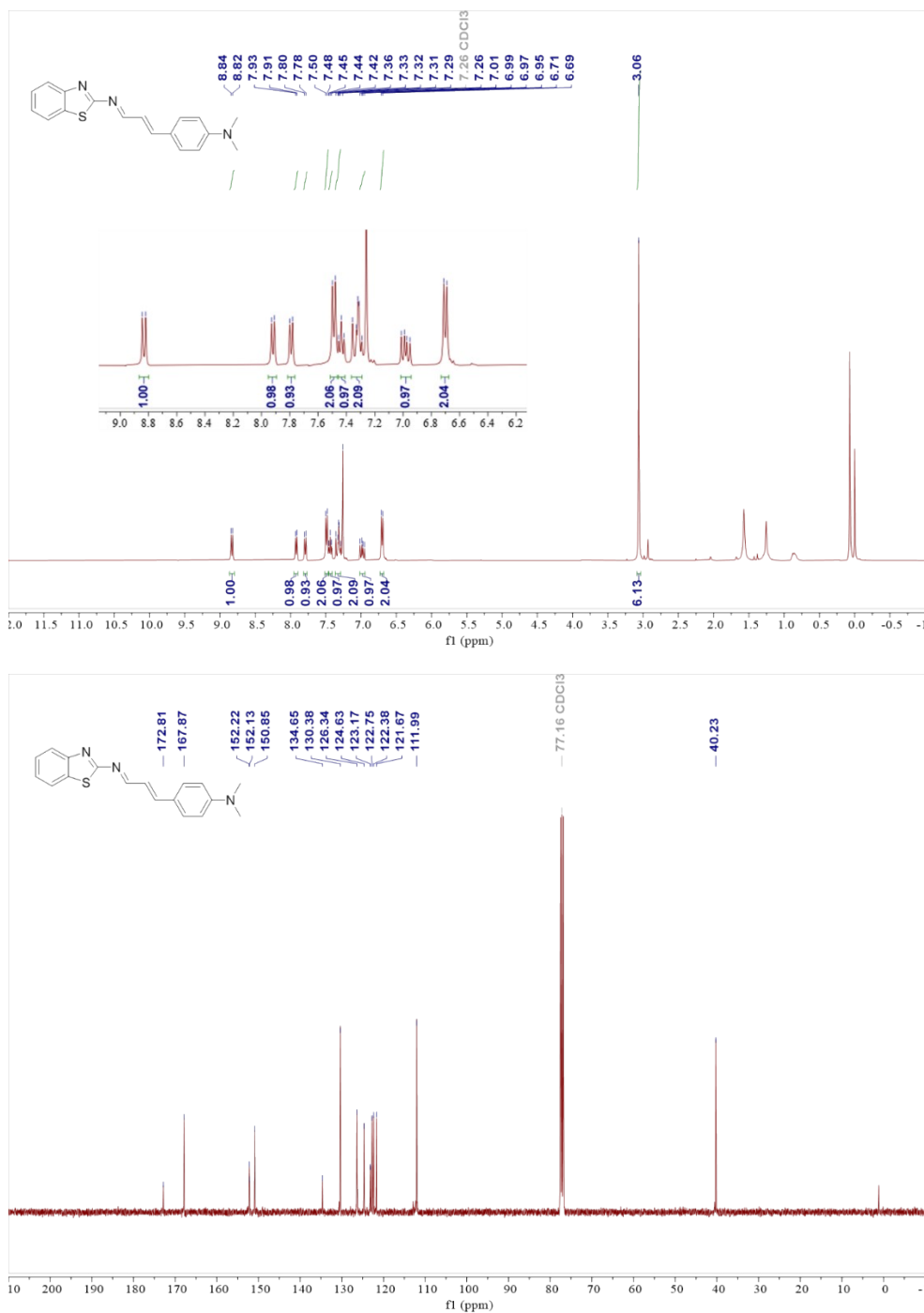


Fig. S9 ^1H NMR, ^{13}C NMR, and HRMS spectra of NC-OH.



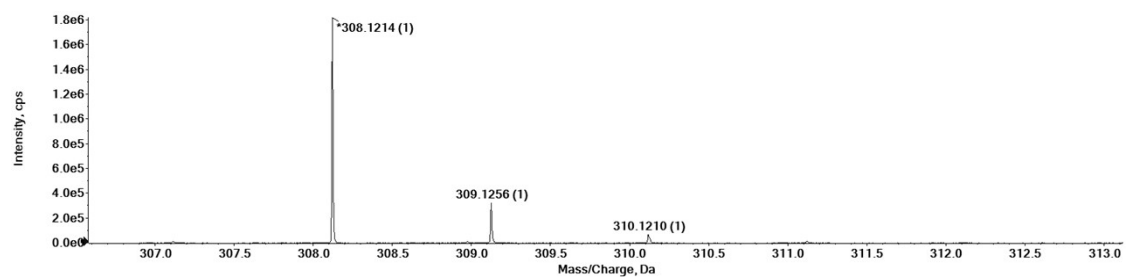
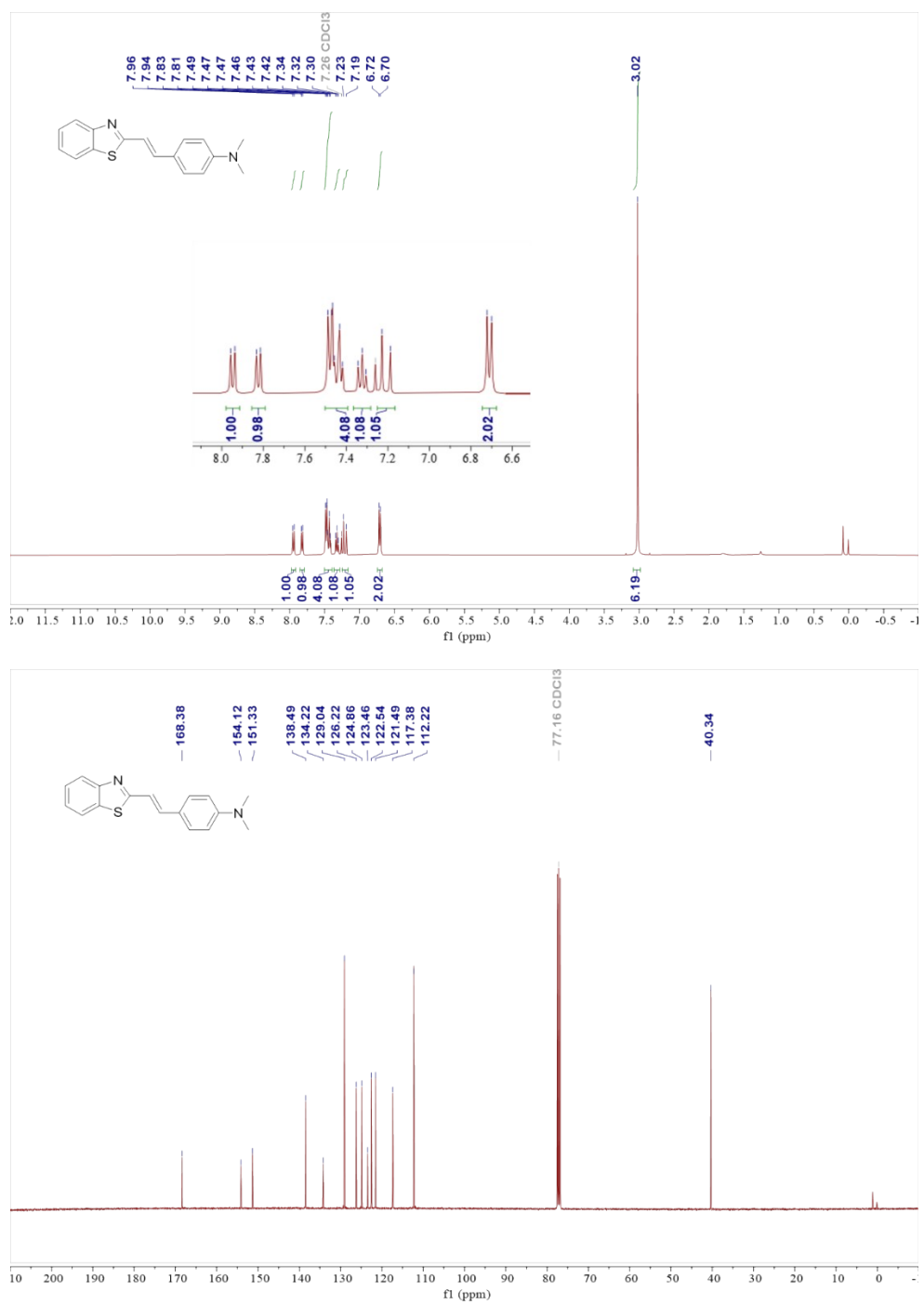


Fig. S10 ^1H NMR, ^{13}C NMR, and HRMS spectra of NCC-Me.



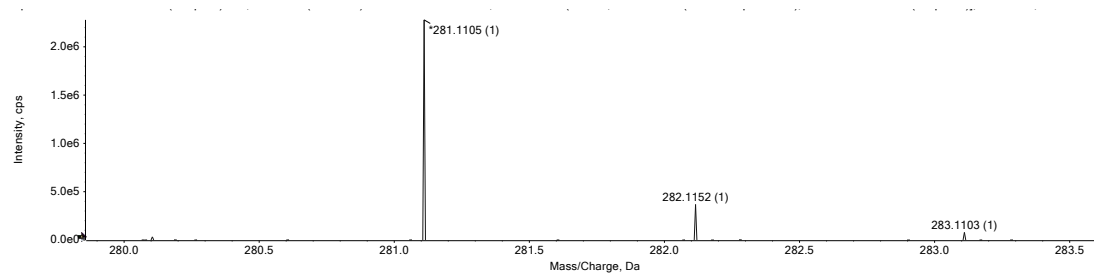
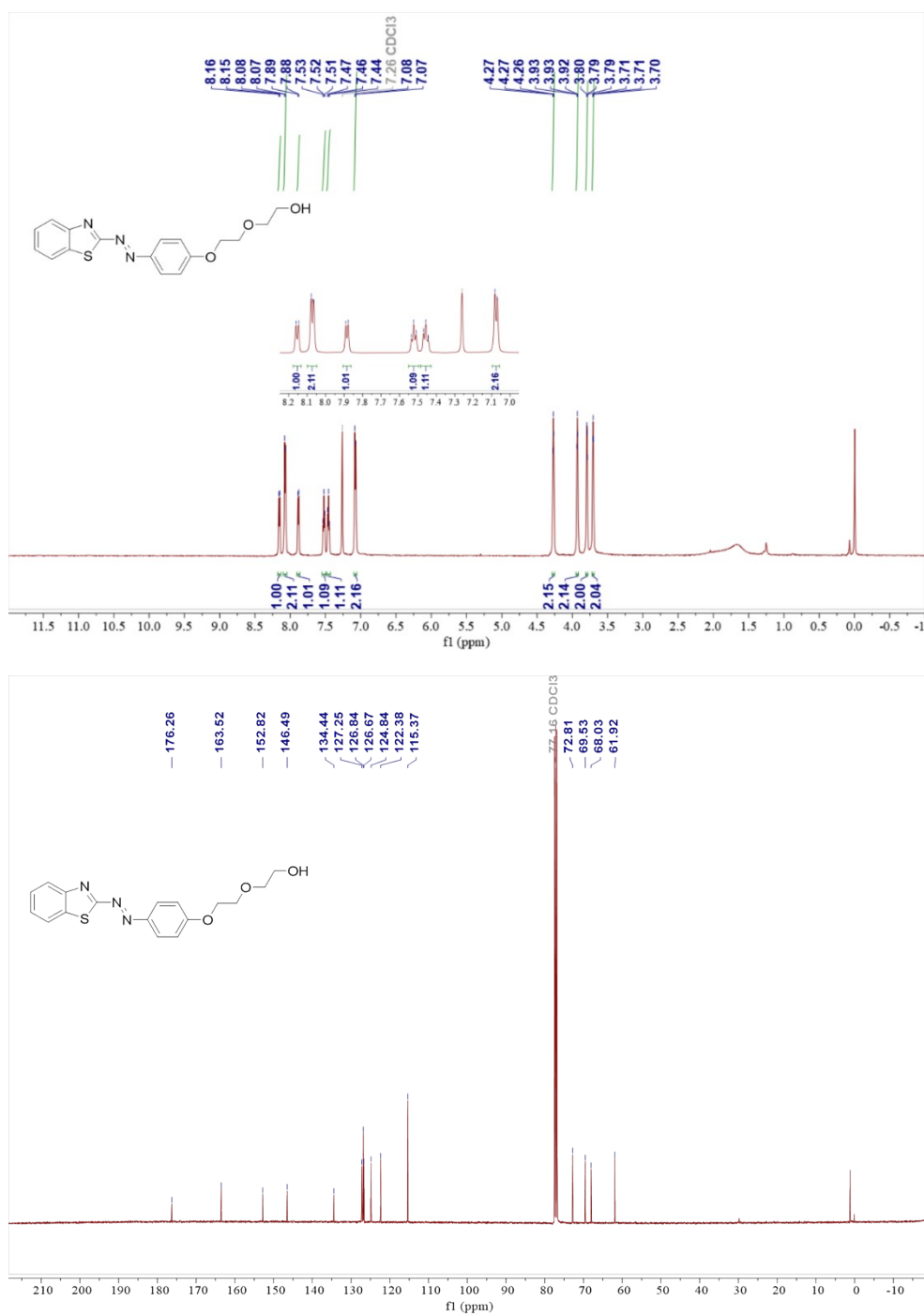


Fig. S11 ^1H NMR, ^{13}C NMR, and HRMS spectra of TZDM-1.



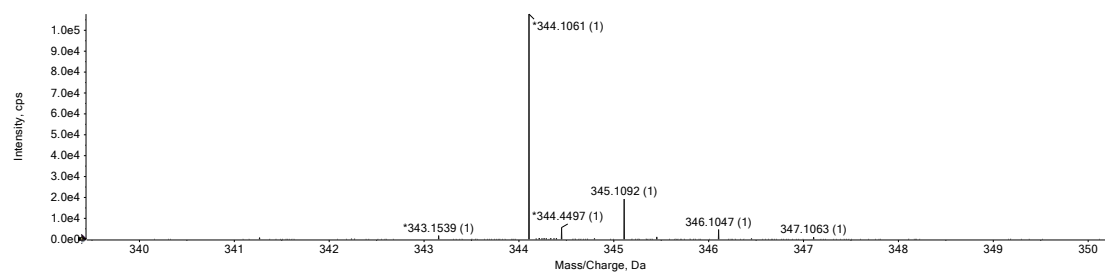
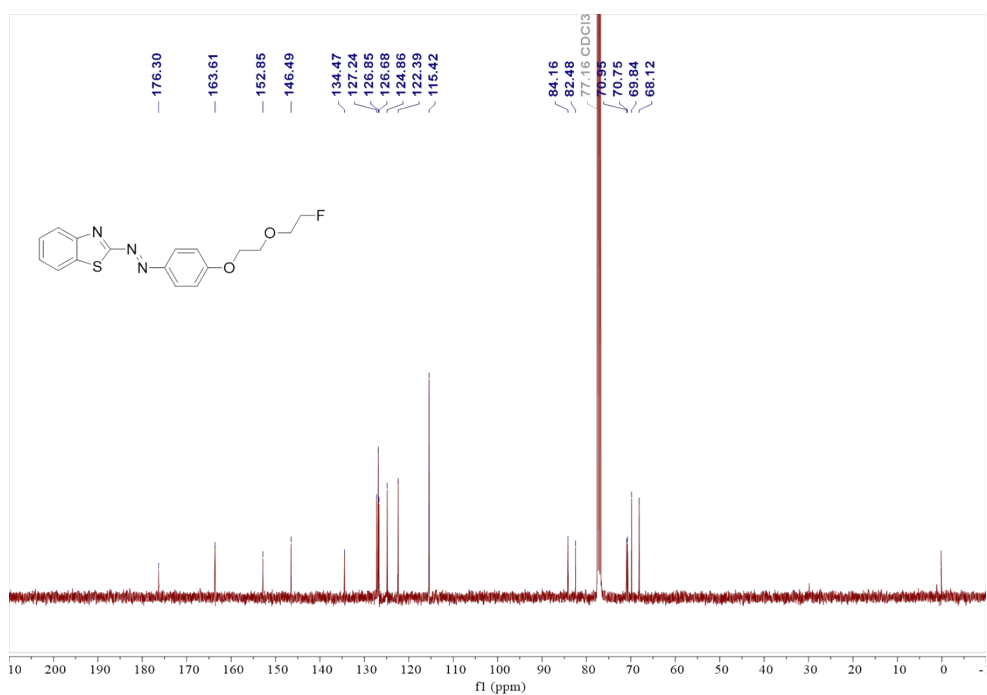
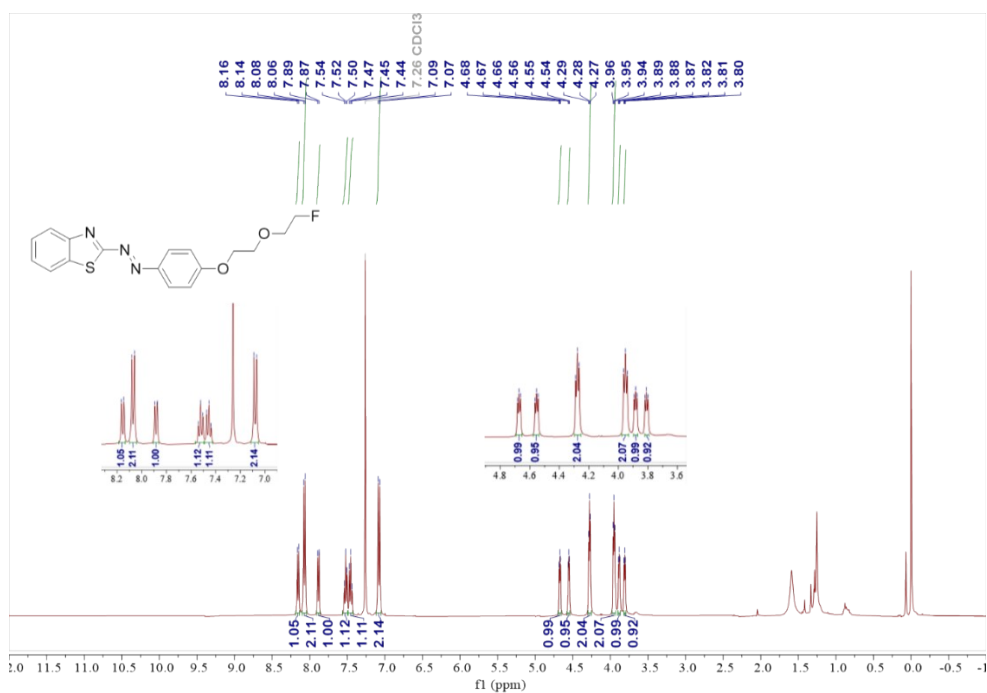


Fig. S12 ^1H NMR, ^{13}C NMR, and HRMS spectra of NN-peg.



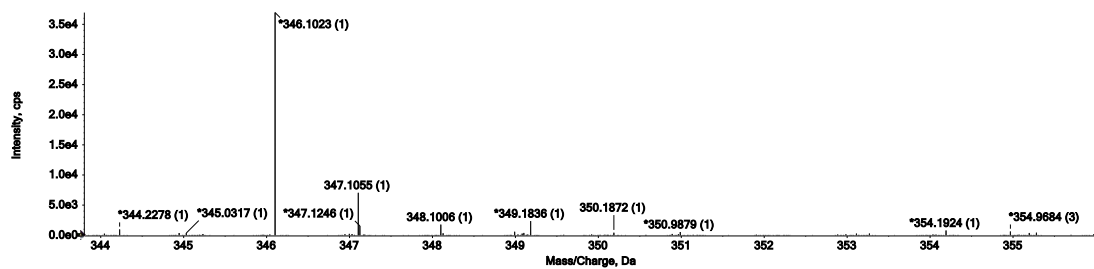
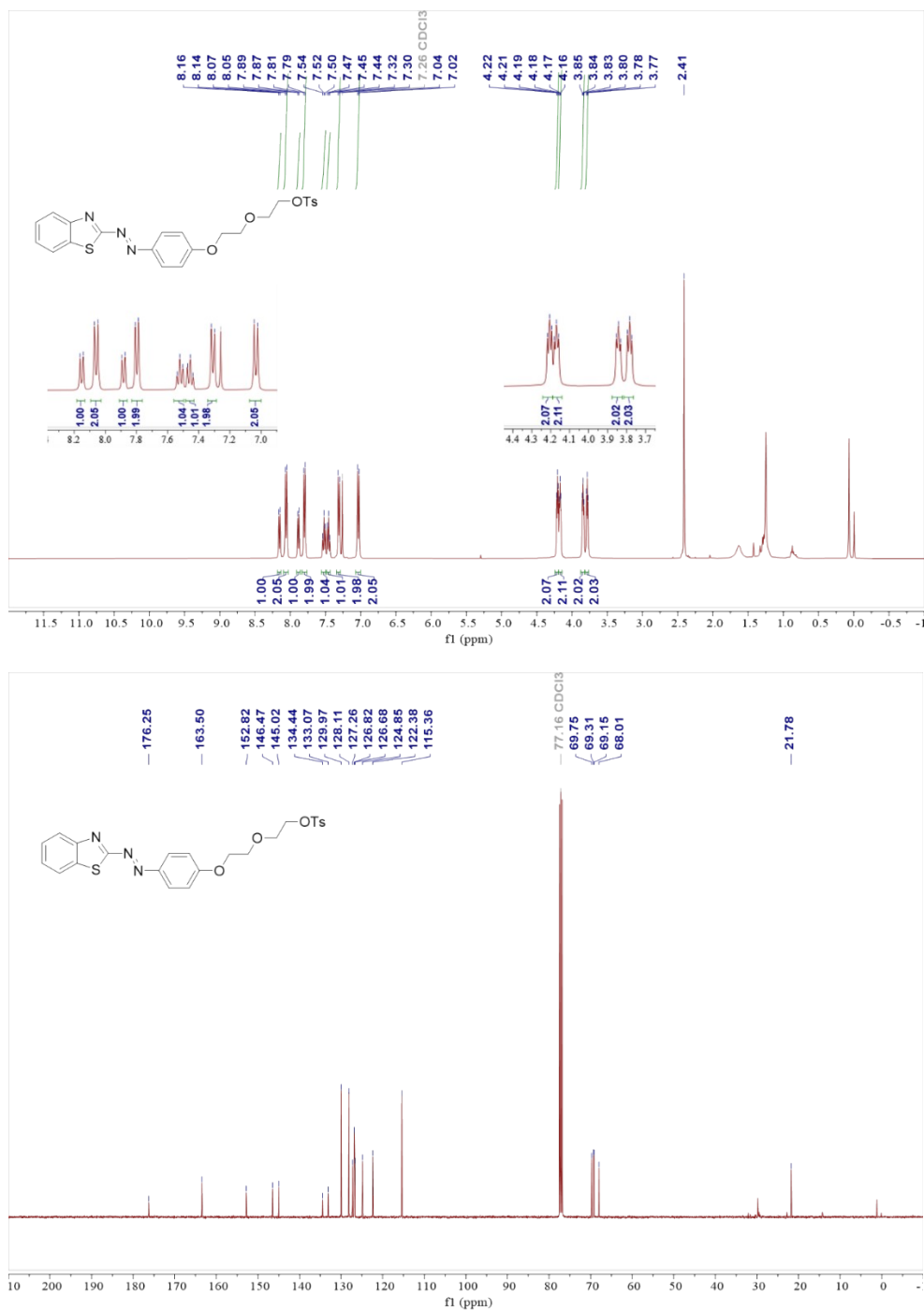


Fig. S13 ^1H NMR, ^{13}C NMR, and HRMS spectra of NN-F.



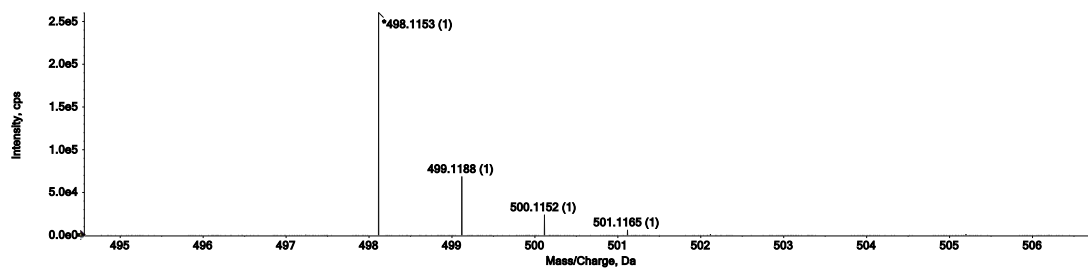


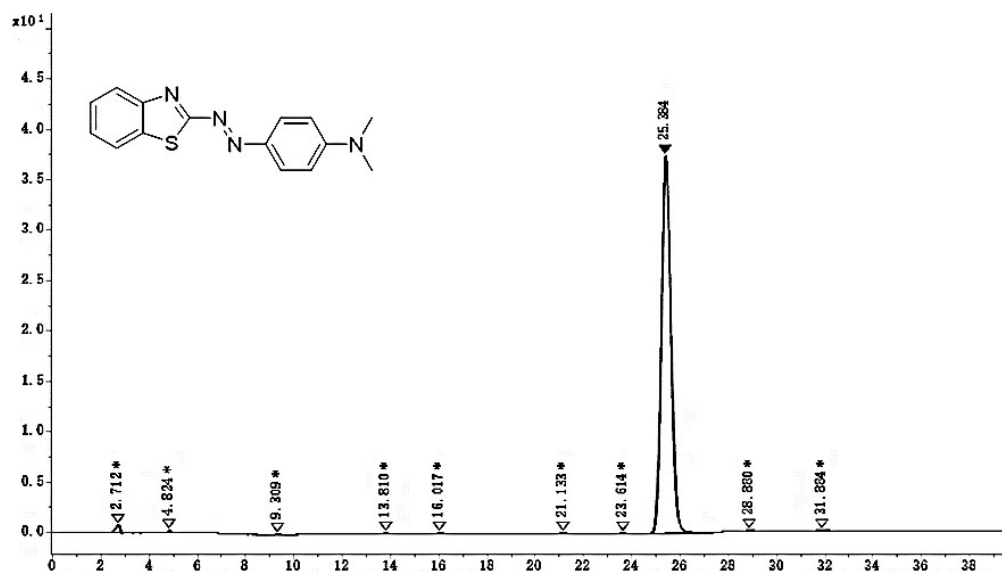
Fig. S14 ^1H NMR, ^{13}C NMR, and HRMS spectra of NN-OTs.

2. HPLC Purity.

Table S1 HPLC purity of the synthesized compounds.

Mobile phase	Mobile phase ration	Flow rate	Compound	Purity (%)
acetonitrile: H ₂ O	60/40	1.0 mL/min	NN-Me	97.68
			NN-OH	99.04
			NiNN-OH	96.56
acetonitrile: H ₂ O	70/30	1.0 mL/min	NN-Et	98.99
			NiNN-Me	95.25
			NiNN-Et	92.61
			TZDM-1	99.94
			NN-F	97.27
			NN-OTs	99.18
acetonitrile: 10 mM aqueous ammonium acetate	80/20	1.0 mL/min	NC-Me	99.73
			NC-Et	98.41
			NC-OH	96.36
			NCC-Me	95.13

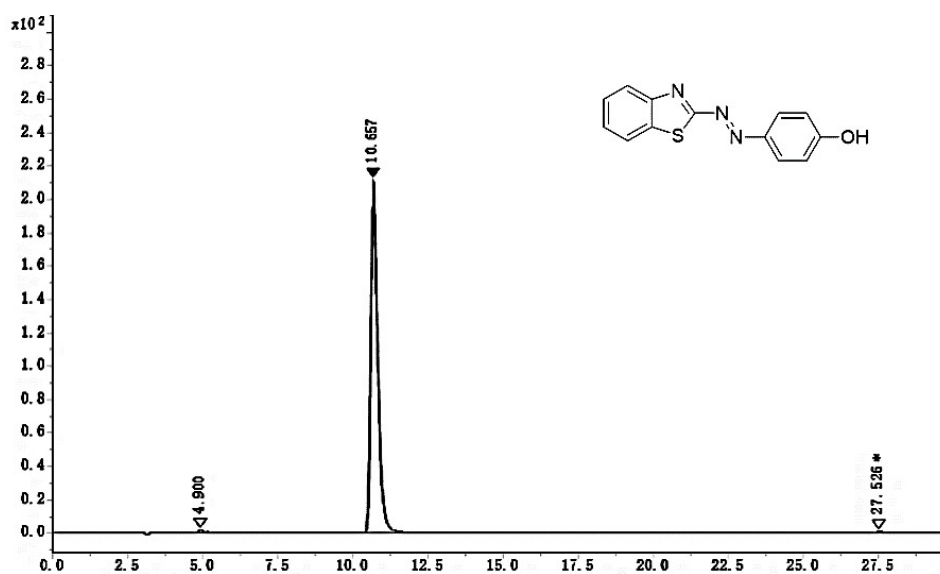
^aHPLC data were obtained from Agilent 1260 system using ZORBAX SB-C18 column (5 μm , 4.6 \times 250 mm). Signals of each compound were investigated by UV-detector under 254 nm.



Peak	Compound	Retention Time/min	AUC/mAU*s	AUC%
1		2.712	9.552	0.92
2		4.824	1.756	0.17
3		9.309	0.73	0.07
4		13.81	1.838	0.18
5		16.017	1.465	0.14
6		21.133	2.205	0.21
7		23.614	0.949	0.09
8	NN-Me	25.384	1009.407	97.68
9		28.88	2.867	0.28
10		31.884	2.717	0.26
Total			1033.486	100.00



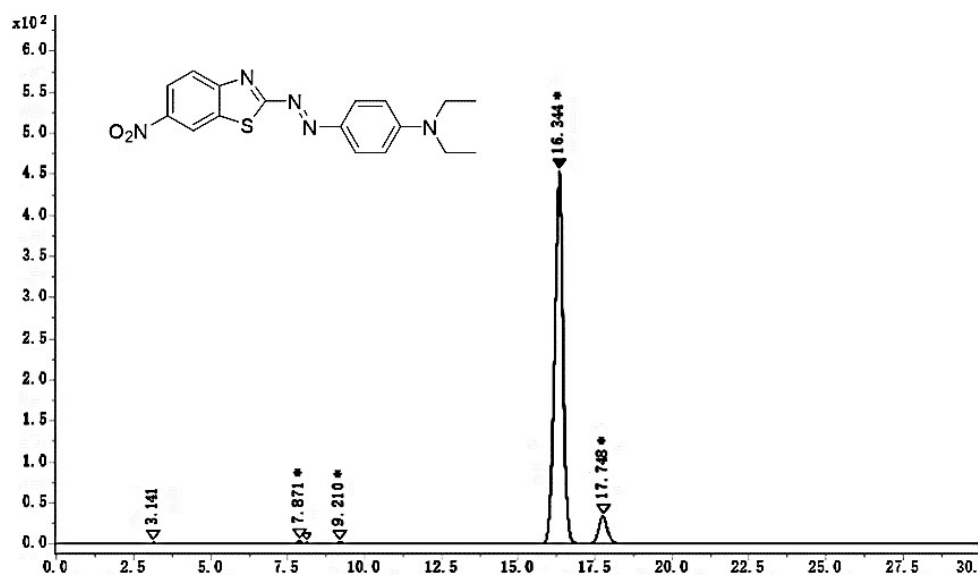
Peak	Compound	Retention Time/min	AUC/mAU*s	AUC%
1		2.503	6.977	0.08
2		3.979	55.53	0.64
3	NN-Et	21.761	8609.666	98.99
4		24.633	25.615	0.29
Total			8697.788	100.00



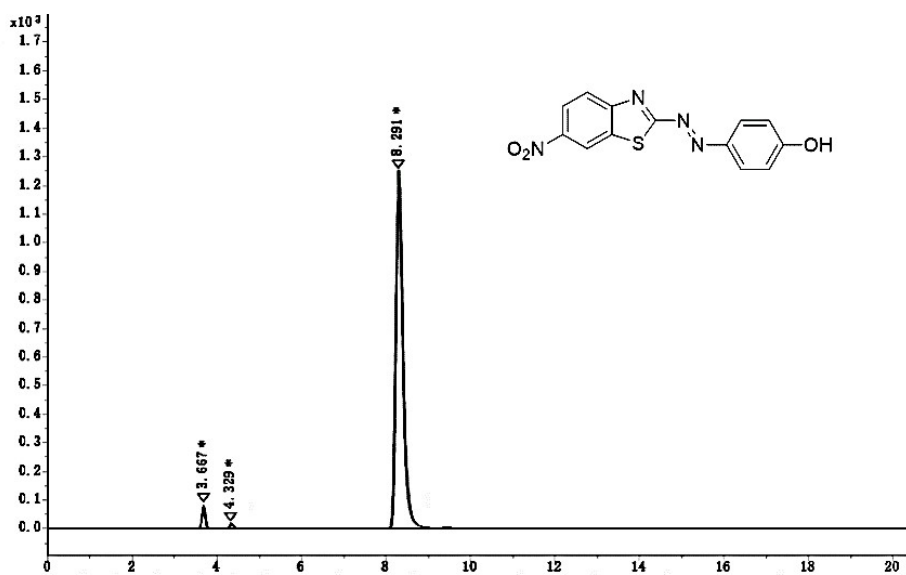
Peak	Compound	Retention Time/min	AUC/mAU*s	AUC%
1		4.9	22.642	0.66
2	NN-OH	10.657	3384.986	99.04
3		27.526	10.293	0.30
Total			3417.921	100.00



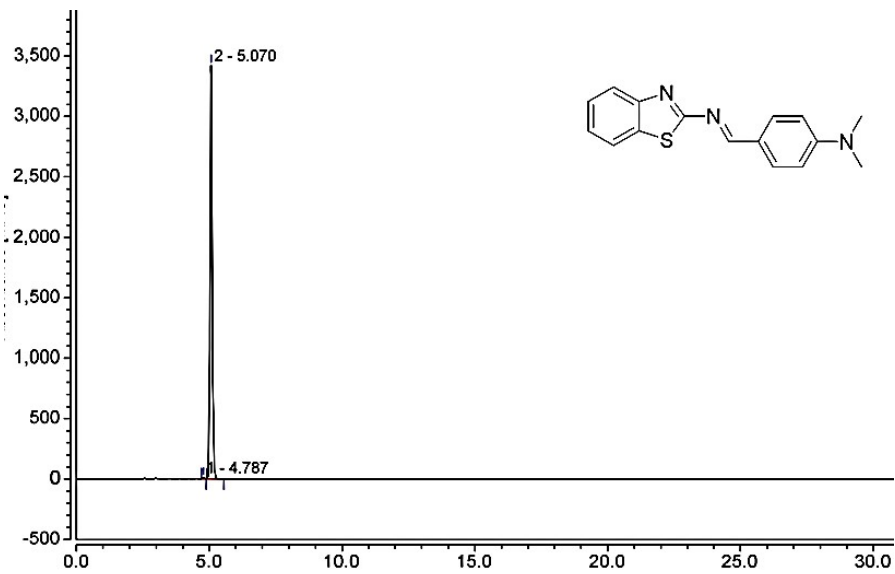
Peak	Compound	Retention Time/min	AUC/mAU*s	AUC%
1		5.041	19.668	1.00
2		5.88	9.333	0.47
3		7.058	15.054	0.76
4		7.73	6.136	0.31
5		8.115	2.485	0.13
6		8.306	21.839	1.11
7		9.438	19.118	0.97
8	NiNN-Me	10.435	1873.494	95.25
Total			1967.127	100.00



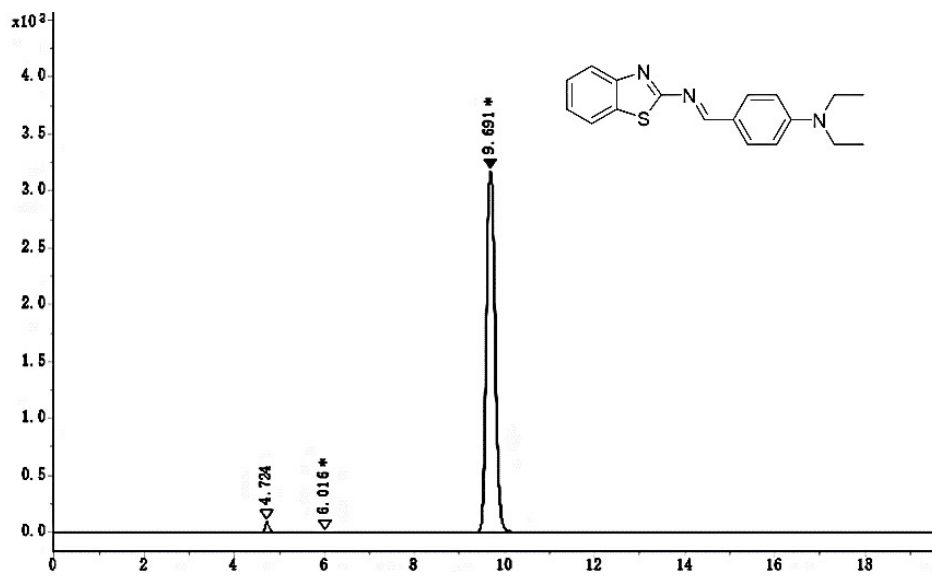
Peak	Compound	Retention Time/min	AUC/mAU*s	AUC%
1		3.141	9.64	0.10
2		7.871	27.136	0.30
3		8.131	5.049	0.06
4		9.21	12.028	0.13
5	NiNN-Et	16.344	8512.239	92.61
6		17.748	625.281	6.80
Total			9191.373	100.00



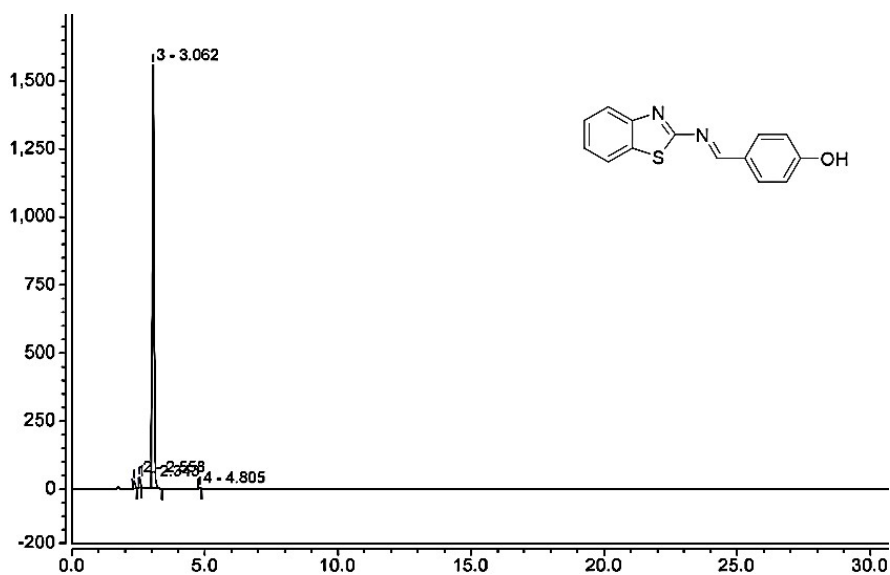
Peak	Compound	Retention Time/min	AUC/mAU*s	AUC%
1		3.667	412.907	2.77
2		4.329	100.380	0.67
3	NiNN-OH	8.291	14417.818	96.56
Total			14931.105	100.00



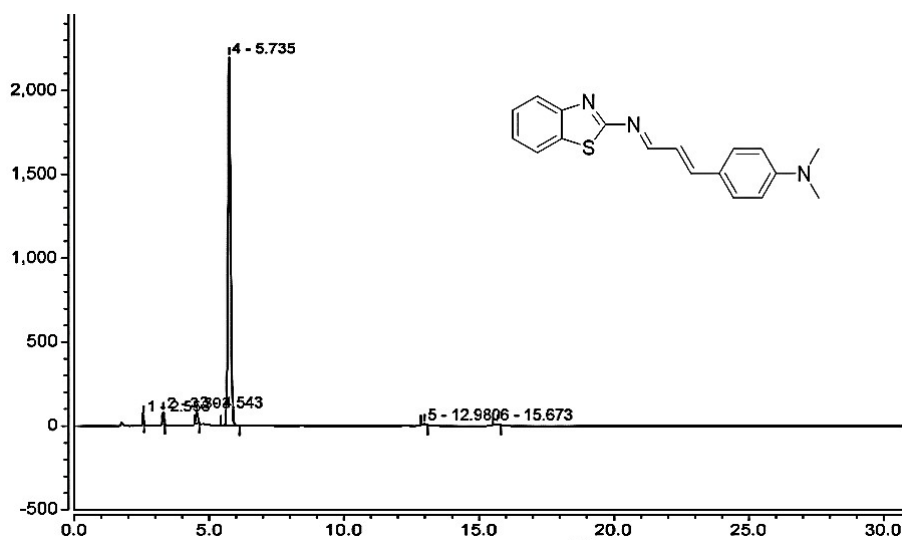
Peak	Compound	Retention Time/min	AUC/mAU*min	AUC%
1		4.787	0.869	0.27
2	NC-Me	5.070	320.521	99.73
Total			3429.990	100.00



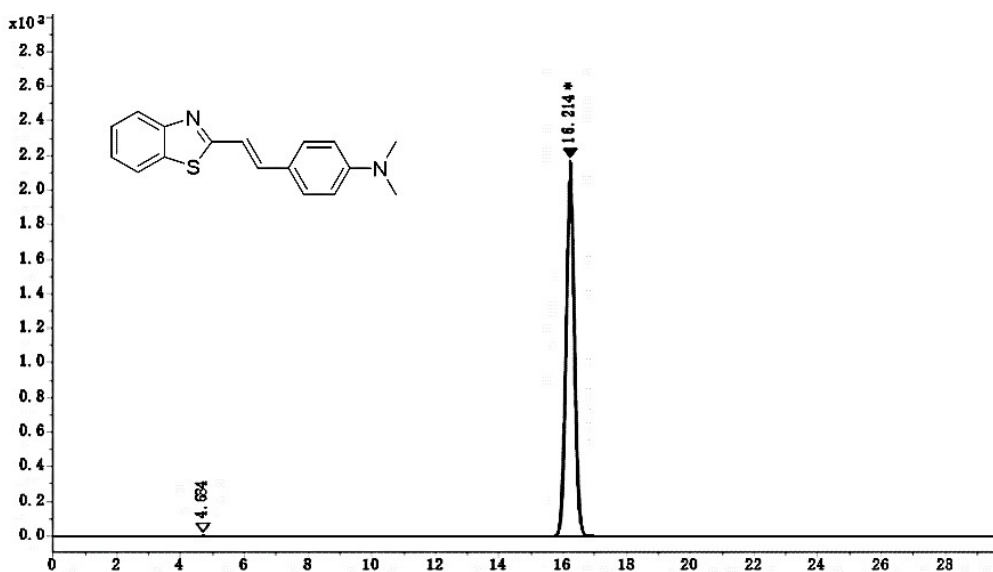
Peak	Compound	Retention Time/min	AUC/mAU*s	AUC%
1		4.723	661.218	1.53
2		6.017	24.534	0.06
3	NC-Et	9.687	42410.239	98.41
Total			43095.991	100.00



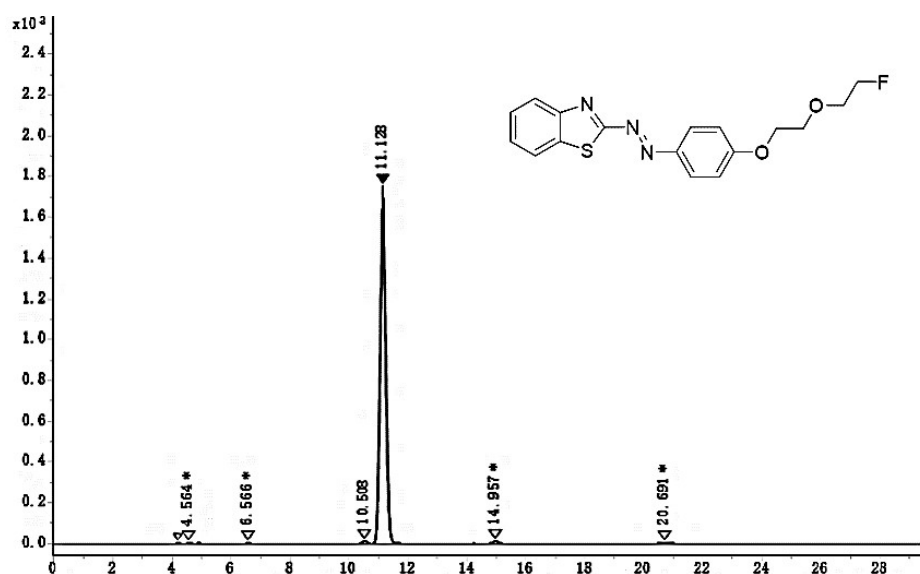
Peak	Compound	Retention Time/min	AUC/mAU*min	AUC%
1		2.343	1.531	1.56
2		2.558	1.666	1.69
3	NC-OH	3.062	94.812	96.36
4		4.805	0.384	0.39
Total			98.394	100.00



Peak	Compound	Retention Time/min	AUC/mAU*min	AUC%
1		2.558	1.379	0.56
2		3.303	3.553	1.43
3		4.543	5.336	2.15
4	NCC-Me	5.735	235.690	95.13
5		12.980	0.766	0.31
6		15.673	1.027	0.41
Total			247.751	100.00



Peak	Compound	Retention Time/min	AUC/mAU*s	AUC%
1		4.684	21.173	0.06
2	TZDM-1	16.214	37955.211	99.94
Total			37976.384	100.00



Peak	Compound	Retention Time/min	AUC/mAU*s	AUC%
1		4.195	38.84	0.17
2		4.564	74.734	0.33
3		6.566	16.365	0.07
4		10.508	172.511	0.76
5	NN-F	11.128	22082.733	97.27
6		14.957	152.61	0.67
7		20.691	165.182	0.73
Total			22702.975	100.00

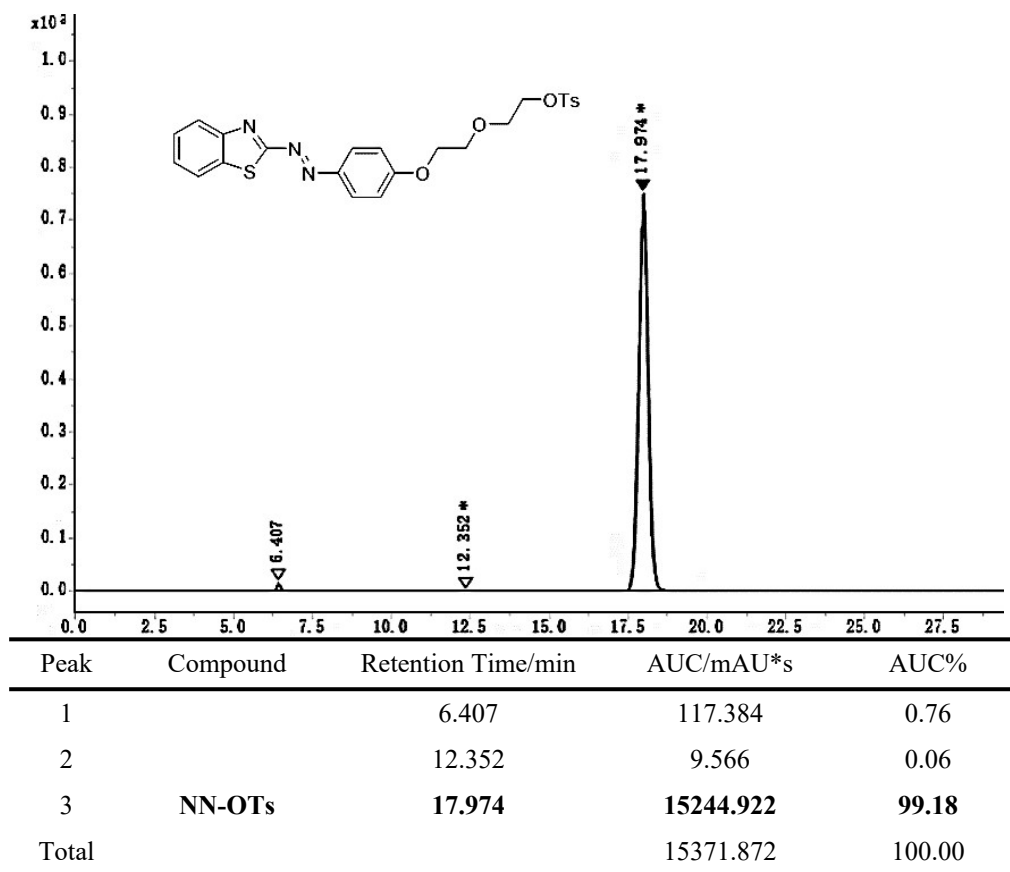


Fig. S15 HPLC data of compounds.

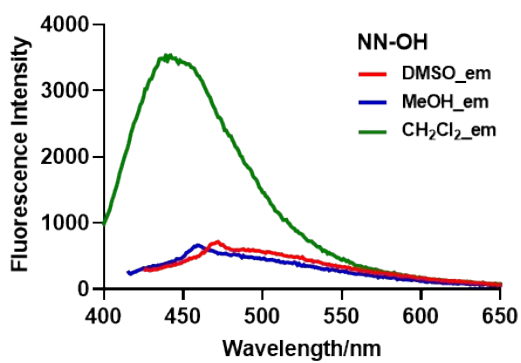
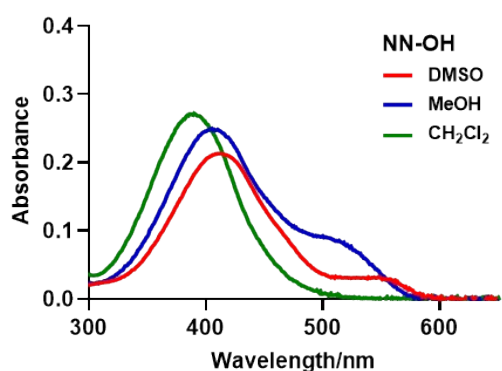
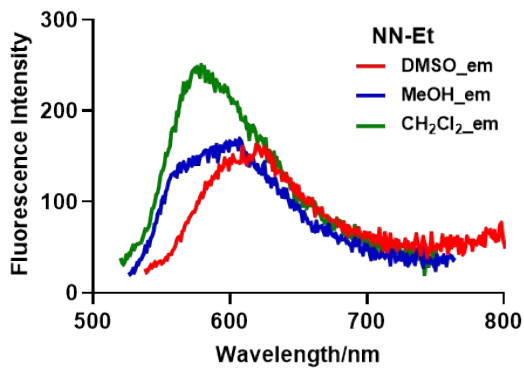
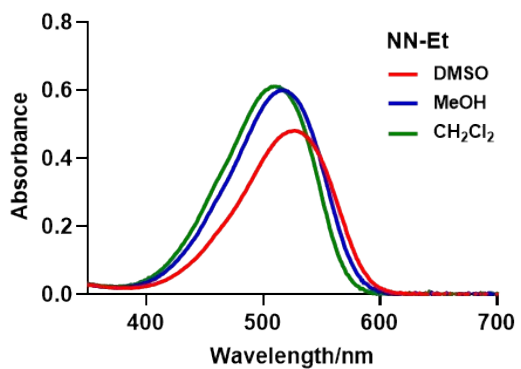
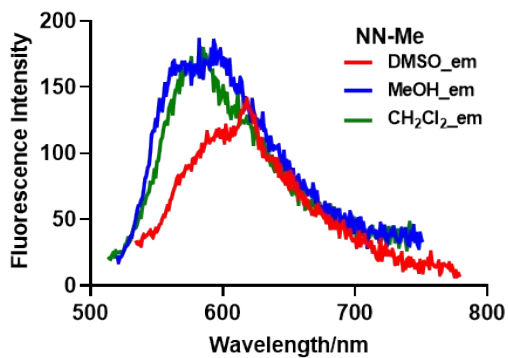
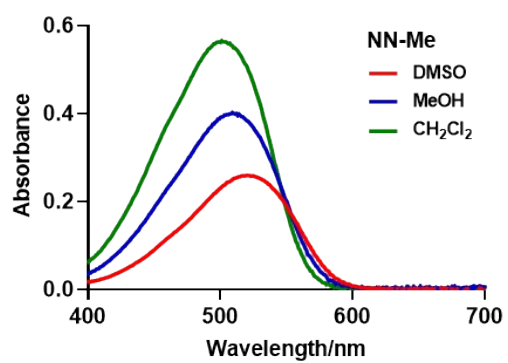
3. Optical Measurements.

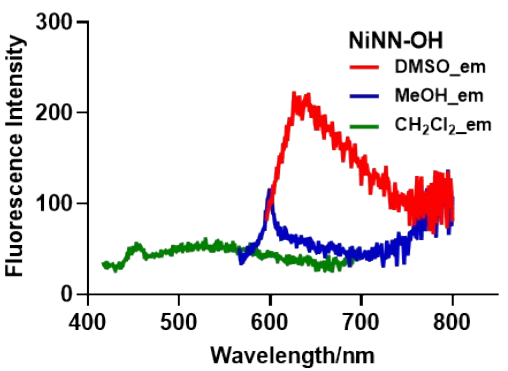
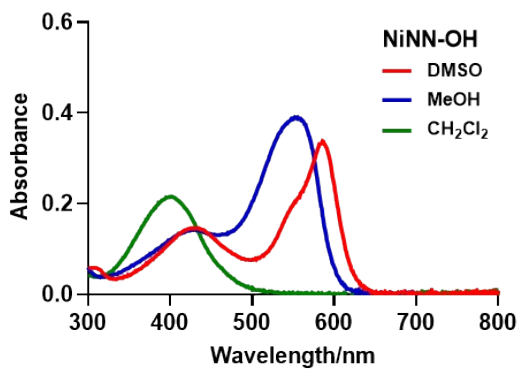
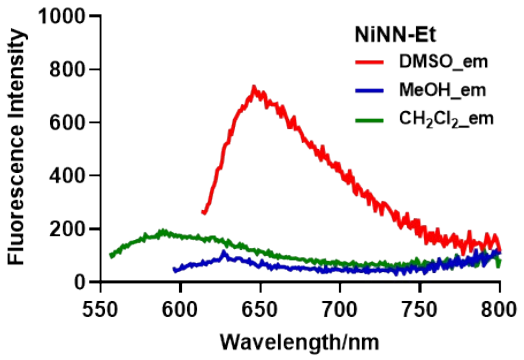
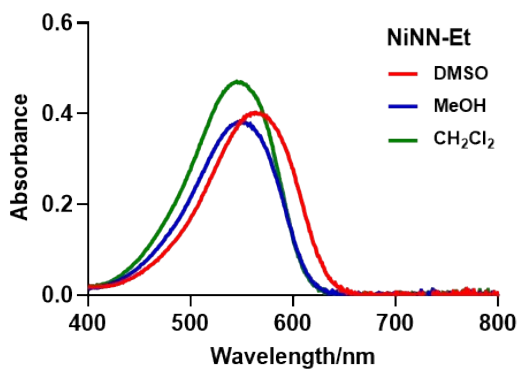
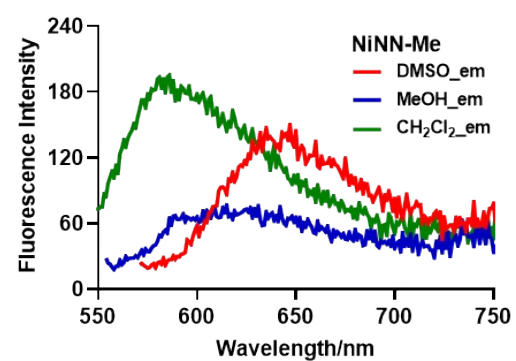
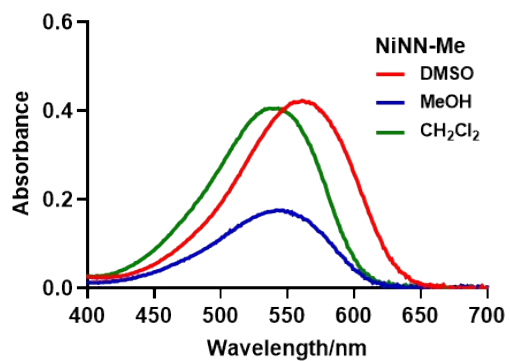
Table S2 Basic properties of compounds.

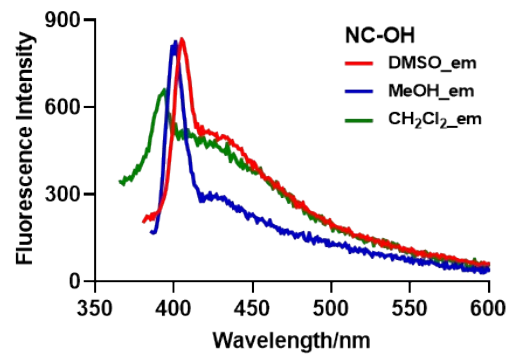
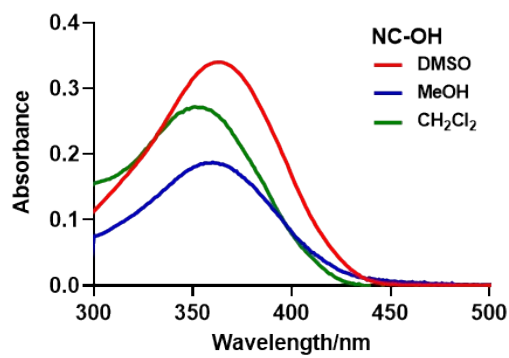
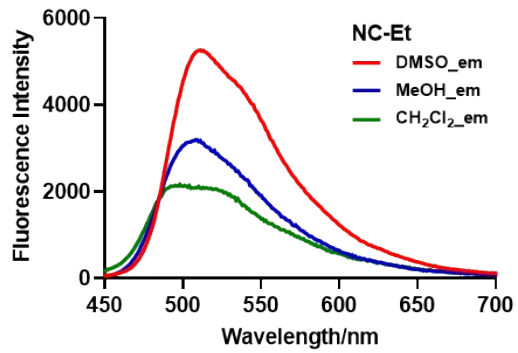
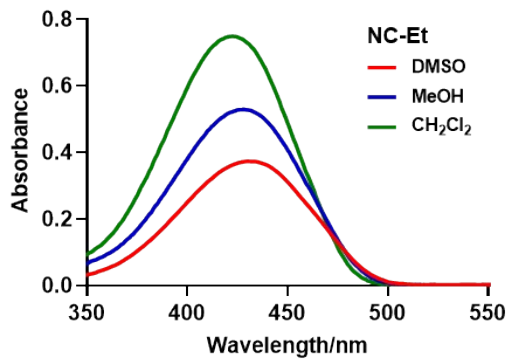
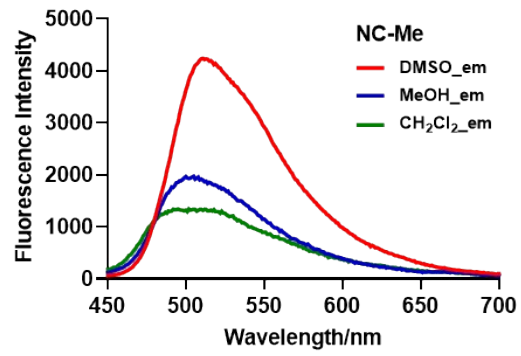
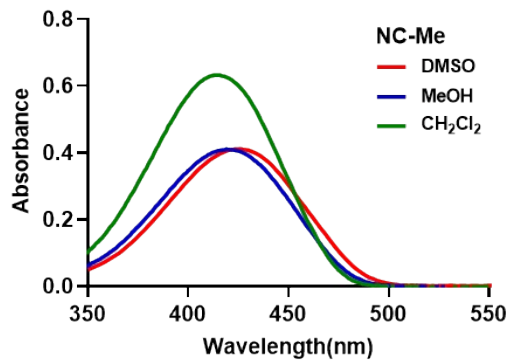
compound	Solvent ^a	λ_{abs}^b (nm)	λ_{ex}^b (nm)	λ_{em}^b (nm)	Stokes shift	ϵ^b (L·M ⁻¹ ·cm ⁻¹)	Φ^c (%)
NN-Me	CH ₂ Cl ₂	502	503	577	74	54 420	0.05
	MeOH	509	510	596	86	40 630	
	DMSO	520	525	618	93	25 690	
	PBS	548	554	672	118	14 080	
NN-Et	CH ₂ Cl ₂	510	511	576	65	55 540	0.05
	MeOH	517	517	606	89	49 910	
	DMSO	527	528	622	94	47 710	
	PBS	545	547	667	120	11 880	
NN-OH	CH ₂ Cl ₂	389	390	433	43	20 390	0.57
	MeOH	406	407	458	51	21 620	
	DMSO	413	416	470	54	20 980	
	PBS	512	515	620	105	32 560	
NiNN-Me	CH ₂ Cl ₂	539	540	584	44	44 490	0.06
	MeOH	545	545	625	80	14 760	
	DMSO	561	562	645	83	25 810	
	PBS	451	455	536	81	17 270	
NiNN-Et	CH ₂ Cl ₂	546	547	580	33	44 970	0.05
	MeOH	548	585	628	43	42 000	
	DMSO	563	605	646	41	39 650	
	PBS	515	583	625	42	20 540	
NiNN-OH	CH ₂ Cl ₂	401	402	455	53	23 350	0.04
	MeOH	554	556	599	43	29 080	
	DMSO	586	587	630	43	30 560	
	PBS	548	548	590	42	46 170	
NC-Me	CH ₂ Cl ₂	415	421	500	79	50 890	0.14

	MeOH	420	428	505	77	38 090	
	DMSO	424	424	509	85	413 00	
	PBS	430	432	505	73	29 090	
NC-Et	CH ₂ Cl ₂	422	426	498	72	63 730	0.13
	MeOH	428	447	509	62	53 640	
	DMSO	430	432	510	78	37 220	
	PBS	438	438	512	74	15 200	
NC-OH	CH ₂ Cl ₂	351	353	393	40	22 130	0.83
	MeOH	360	360	401	41	18 700	
	DMSO	364	364	405	41	33 800	
	PBS	384	388	443	55	19 210	
NCC-Me	CH ₂ Cl ₂	449	473	580	107	44 670	0.11
	MeOH	461	483	596	113	45 650	
	DMSO	462	462	600	138	43 270	
	PBS	405	471	606	135	21 770	
TZDM-1	CH ₂ Cl ₂	397	397	489	92	23 270	0.68
	MeOH	401	401	514	113	26 700	
	DMSO	406	409	521	112	23 760	
	PBS	351	392	538	146	18 430	

^aPBS represents spectra of each compound (1 μ M) detected in PBS solutions (pH 7.4, containing 5% DMSO), while CH₂CH₂, MeOH, DMSO represent spectra of each compound (10 μ M) detected in respective organic solvents. ^b λ_{abs} , λ_{ex} , λ_{em} , and ϵ represent maximum absorption wavelength, maximum excitation wavelength, maximum emission wavelength, and molar absorption coefficient, respectively. ^c Φ represents fluorescence quantum yield (%) of respective compounds (1 μ M) in CH₂Cl₂.







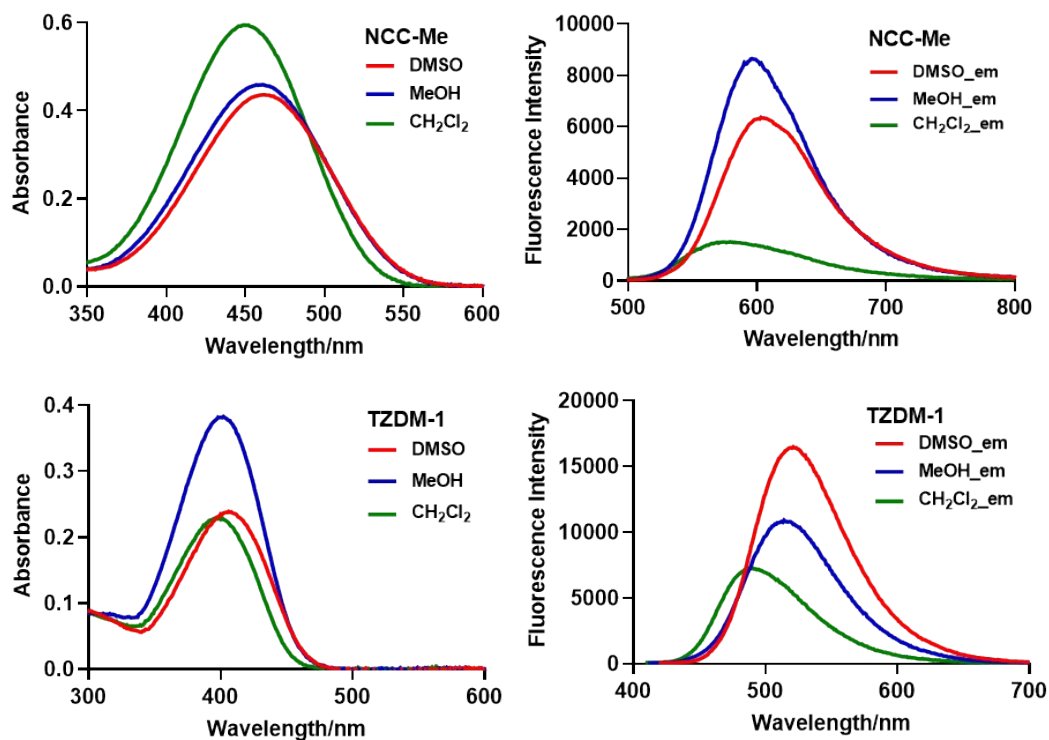


Fig. S16 Absorption spectra (left) and fluorescence emission spectra (right) of compounds (10 μ M) in different solvents.

4. Preparation of Protein Aggregates.

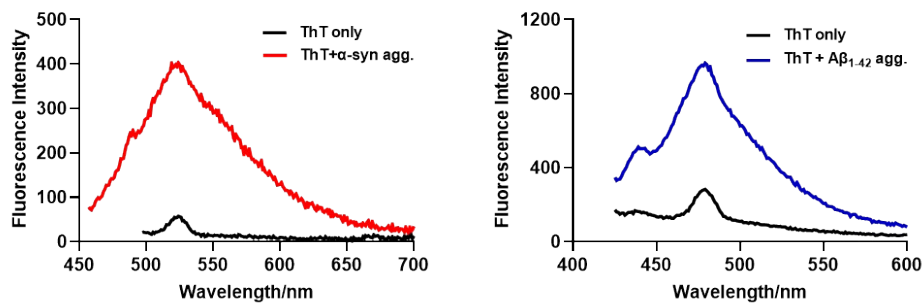


Fig. S17 Confirmation of protein aggregation by thioflavin T (ThT) in PBS solutions (pH = 7.4, containing 4% ethanol).

5. Spectral Measurements with Protein Aggregates in Solutions.

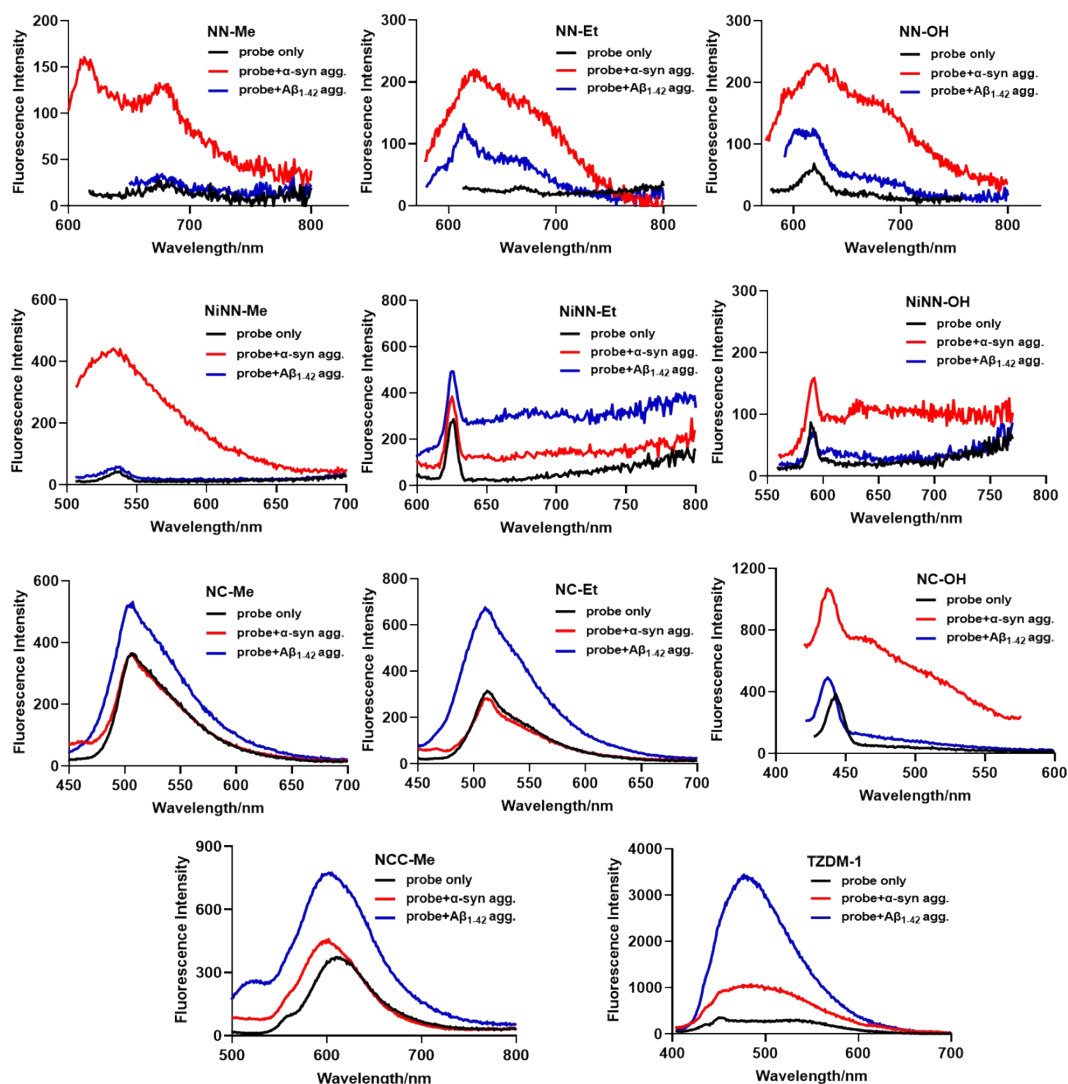


Fig. S18 Fluorescence spectra of each compound (1 μM) upon mixing with protein aggregates (2.75 μM) in PBS solutions (pH = 7.4, containing 5% DMSO).

6. Fluorescence staining.

Compounds with N=N linkage were evaluated towards pathological α -syn aggregates using 16- μm -thick frozen brain slices from an aged A53T-Tg mouse (24-month-old, male). Fluorescent images were observed after the addition of each compound to respective brain slices, and aggregated α -syn pathology was confirmed by immunostaining with Syn 505 antibody.^{1, 2} To be more specific, brain slices were incubated with each compound (50 μM , 50% ethanol) for 20 min, dried at room temperature after 2×1 min washes in 50% ethanol.³ To confirm the presence of aggregated α -syn pathology, the same slices were first treated with 0.1% Triton X-

100 in PBS solutions (0.01 M, pH = 7.4) for permeabilization for 5 min and washed with PBS solutions. After drying, the slices were incubated with normal goat serum for blocking at room temperature for 1.5 h, then washed with PBS solutions. The slices were next incubated with an anti- α -syn monoclonal antibody (1:1000, Syn 505, Invitrogen, USA) at 4°C for 20 h. After that, the slices were incubated with Alexa Fluor 488-conjugated secondary antibody (1:500, Beyotime, China) at 37°C for 1.5 h after 3 \times 5 min washes in PBS-Tween 20 solutions (0.3% Tween 20), followed by another three washes, and were finally observed on the EVOS FL imaging system (Life, USA) equipped with standard filter sets of GFP and RFP. For fluorescence staining of **NN-F**, 16- μ M-thick frozen brain slices from the aged A53T-Tg mouse (24-month-old, male) and 8- μ M-thick deparaffinized slices from a PD patient (80-year-old, female) were used. Of note, paraffin-embedded brain slices were first deparaffinized with 2 \times 10 min washes in xylene, 2 \times 2 min washes in 100% ethanol, 2 min wash in 90% ethanol/water, 2 min wash in 80% ethanol/water, 2 min wash in 70% ethanol/water, 2 \times 2 min washes in water, and then were allowed to dry at room temperature. Brain slices were incubated with **NN-F** (50 μ M, 50% ethanol) for 20 min, then dried at room temperature after 2 \times 1 min washes in 50% ethanol. The same slices were also conducted to immunostaining using Syn 505 antibody. Differently, an Alexa Fluor 647-conjugated secondary antibody (1:500, Beyotime, China) was used and images were obtained from SLIDEVIEW VS200 scanning system (Olympus, Japan) equipped with DAPI, FITC, and CY5 filters.

As shown in Figure S19, fluorescent labeling of **NN-OH** colocalized well with Syn505 immunofluorescence, while **NN-Me** and **NN-Et** showed obvious nonspecific staining on the brain tissue. Notably, **NiNN-Me** and **NiNN-Et** with nitro group displayed improved colocalization with Syn505 antibody compared to **NN-Me** and **NN-Et**, indicative of the effectiveness of nitro group for α -syn binding. The neuropathological staining results were consistent with the results for α -syn aggregates in solution in vitro, suggesting that benzothiazole derivative with N=N linkage could bind to pathological α -syn aggregates as well as α -syn aggregates in solution.

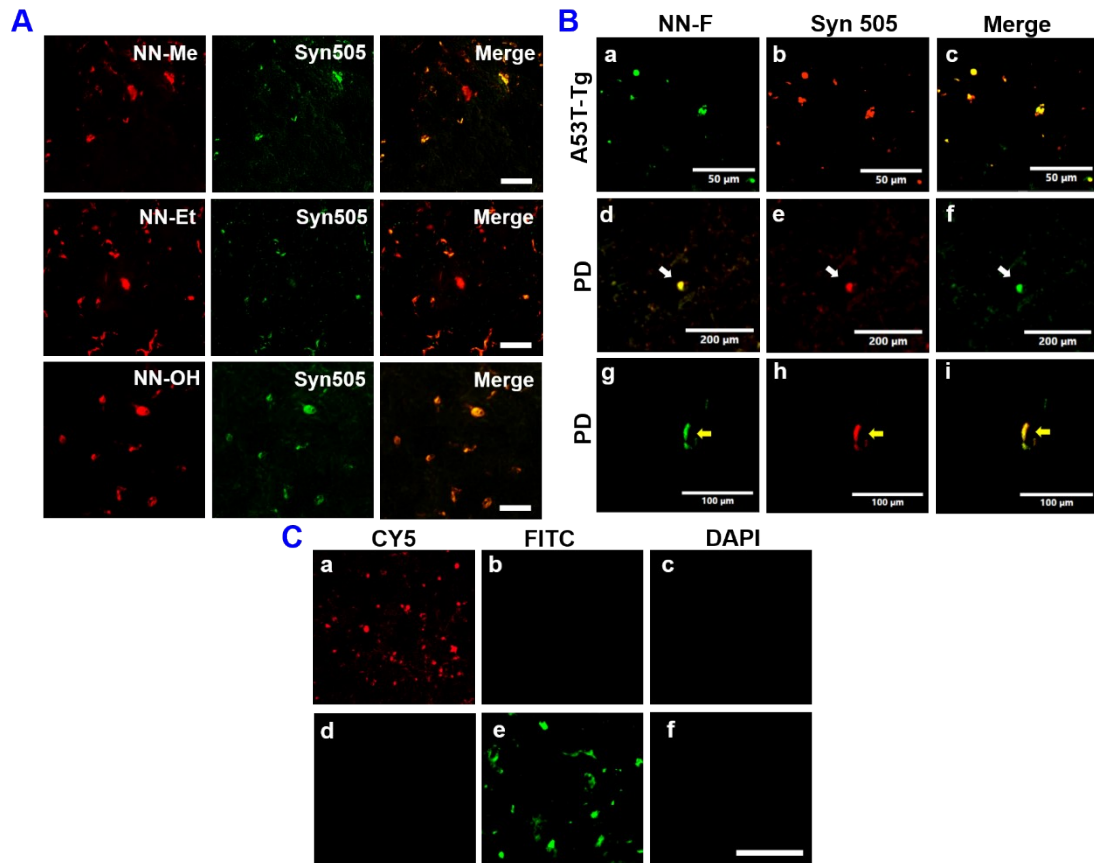


Fig. S19 (A) Double staining of α -syn pathology in an A53T-Tg mouse (24-month-old, male) with NN series (50 μ M, 50% ethanol) and Syn 505 monoclonal antibody. Scale bar = 20 μ M. (B) Double staining of α -syn pathology in the A53T-Tg mouse (24-month-old, male) and a PD patient (80-year-old, female) with NN-F (50 μ M, 50% ethanol) and Syn 505 monoclonal antibody. LBs: white arrow head; LNs: yellow arrow head. Scale bar = 50 μ M. (a-c), 200 μ M (d-f), 100 μ M (g-i). NN-F efficiently labeled pathological α -syn aggregates in brain tissue from aged A53T-Tg mouse and in PD brain tissue. (C) Immunostaining of α -syn pathology in the A53T-Tg mouse brain (24-month-old, male) with Syn 505 monoclonal antibody. (a-c) Syn 505 + Alexa Fluor 647-conjugated secondary antibody; (d-f) Syn 505 + Alexa Fluor 488-conjugated secondary antibody. Scale bar = 200 μ M.

7. Saturation Binding Assays of NN-F.

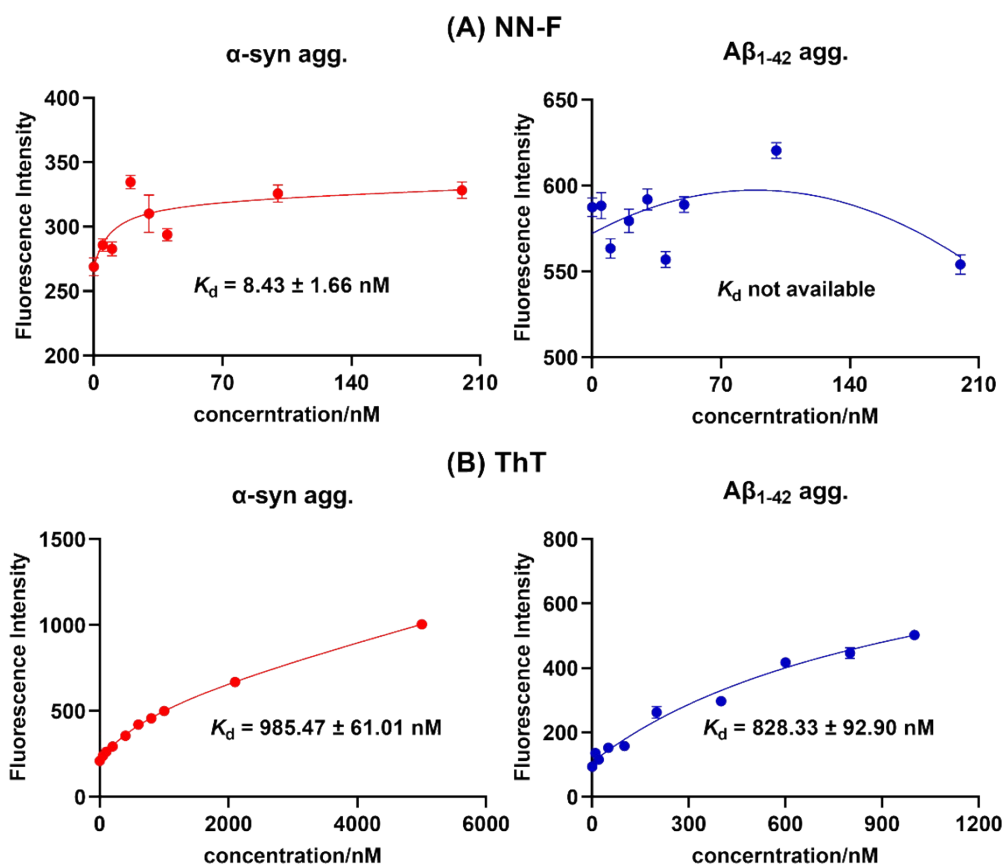


Fig. S20 Saturation curves of NN-F and ThT with protein aggregates in PBS solutions (pH = 7.4, containing 5% DMSO).

8. Stability Studies.

Table S3 Stability of [^{18}F]NN-F in the mouse plasma.

	NO.	Retention time (min) ^a	Concentration (%)
30 min	1	4.612	6.94
	2	7.353	93.06
60 min	1	4.888	5.21
	2	7.505	91.19
	3	3.704	3.60

^aHPLC profiles were obtained from Agilent 1100 system equipped with UV-vis and γ -detector, using ZORBAX SB-C18 column (5 μm , 4.6 \times 250 mm) with mobile phase at a flow rate of 1.0 mL/min.

Table S4 Stability of NN-F in acetonitrile.

	NO.	Retention time (min) ^a	Concentration (%)
0 min	1	4.318	0.44
	2	8.136	99.56
Daylight-2 h	1	5.087	7.86
	2	8.498	92.14
UV ₂₅₄ -1h	1	5.210	7.75
	2	8.611	92.25
UV ₂₅₄ -2h	1	5.054	7.36
	2	8.451	92.64
Heat	1	5.250	61.25
	2	8.634	38.75
Removal of heat	1	5.047	36.38
	2	8.357	63.62

^aHPLC profiles were obtained from Agilent 1100 system using ZORBAX SB-C18 column (5 μ m, 4.6 \times 250 mm) with mobile phase at a flow rate of 1.0 mL/min. Signals of NN-F were investigated by UV-detector under 254 nm.

References

1. E. A. Waxman, J. E. Duda and B. I. Giasson, *Acta Neuropathologica*, 2008, **116**, 37-46.
2. J. E. Duda, B. I. Giasson, M. E. Mabon, V. M. Y. Lee and J. Q. Trojanowski, *Annals of Neurology*, 2002, **52**, 205-210.
3. H. Watanabe, M. Ono, T. Ariyoshi, R. Katayanagi and H. Saji, *ACS Chemical Neuroscience*, 2017, **8**, 1656-1662.